

MINISTRY OF EDUCATION
AND TRAINING

VIETNAM ACADEMY OF SCIENCE AND TECHNOLOGY

GRADUATE UNIVERSITY OF SCIENCE AND TECHNOLOGY



DAO PHI HUNG

**STUDY ON PREPARATION, STRUCTURAL CHARACTERISTICS
AND PROPERTIES OF MULTIFUNCTIONAL COATING BASED ON
ACRYLIC EMULSION POLYMER AND NANOFILLERS**

Major: Chemistry
Code: 9 44 01 14

SUMMARY OF DOCTORAL THESIS ON CHEMISTRY

Ha Noi, 2023

The thesis was completed at Graduate University of Science and Technology – Vietnam Academy of Science and Technology

Supervisor: Prof. Dr. Thai Hoang

Reviewer 1:

Reviewer 2:

Reviewer 3:

The doctoral thesis will be defended in front of the Doctoral Thesis Evaluation Council, held at the Graduate University of Science and Technology - Vietnam Academy of Science and Technology at ... hour ..', date ... month ... year 2023

The thesis can be found at:

- Library of Graduate University of Science and Technology
- National Library of Vietnam

INTRODCUTION

1. The urgency of the thesis

Global warming has led to an increased demand for cooling energy in buildings. In the context of climate change adaptation and mitigation, many countries worldwide are concerned about reducing CO₂ emissions and enhancing energy security. As a result, there has been growing interest in researching and developing solar reflective paints for buildings. The lifespan of paint coatings significantly depends on the development of microorganisms such as bacteria, yeast, and mold on the paint's surface. Consequently, there is a need for paint systems that can inhibit the growth of these microorganisms to extend the coating's lifespan. Moreover, antibacterial paint coatings have been investigated for their potential to reduce the risk of microbial infections. Currently, the research, development, and refinement of solar reflective and antibacterial coatings represent a research direction with practical importance, relevance, and significant scientific value.

Due to severe environmental pollution, environmental protection laws have been enacted with the purpose of restricting the impact of industrial activities on the environment. Environmentally friendly paint systems, based on non-solvent or waterborne binders, have been researched and developed to reduce the amount of volatile organic compounds. Additionally, paints using waterborne binders not only reduce volatile organic compounds but also enhance fire safety during manufacturing and transportation. Acrylic emulsion polymers are a popular type of waterborne binder. Paint formulas based on acrylic emulsion polymers, with reasonable costs, can produce coatings with excellent weather durability, chemical resistance, and minimal environmental impact. However, acrylic chains are often modified with hydrophilic functional groups to improve the dispersion of acrylic polymer in water. This makes coatings more susceptible to the penetration of air and water, reducing certain properties of acrylic coatings, such as water resistance and anti-corrosion capabilities. These limitations restrict the application fields of acrylic emulsion polymers. To address these limitations and expand the range of applications, ongoing research and development efforts are focused on acrylic emulsion polymers. Consequently, the PhD candidate has chosen the project: "Study on the preparation, structural characteristics, and properties of multifunctional coatings based on acrylic emulsion polymers and nanofillers."

2. Objectives of the thesis

Fabrication a coating based on acrylic emulsion polymers with nanofillers and organic additives that exhibit both solar-reflective and antimicrobial properties is a complex task with several specific objectives:

- Modified TiO₂, ZrO₂ nanoparticles (NPs) with suitable organic coupling agents with the aim of achieving regular dispersion within the acrylic emulsion polymer matrix.
- Evaluate the synergistic effects of organically modified nanofillers on the properties of acrylic coatings, including mechanical properties, thermal stability, and solar reflection. Additionally, assess the synergistic effects of both organic and inorganic antibacterial agents on the antimicrobial properties of the coating.

3. Content of the thesis

The thesis includes:

- TiO₂ NPs were modified with some coupling agents, namely [3-(methacryloyloxy)propyl]trimethoxysilane (TMSPM) and isopropyl tri(dioctylpyrophosphate)titanate (KR-12). Similarly, ZrO₂ NPs were also modified with [3-(methacryloyloxy)propyl]trimethoxysilane (TMSPM) and (3-glycidyoxypropyl)triethoxysilane (GPTES). The primary objectives were to determine the characteristics, properties, and morphology of these modified nanoparticles. Following this, several properties of coatings based on acrylic emulsion polymers and these modified nanoparticles were assessed.
- Effect of modified NPs on properties of nanocomposite coatings, including solar reflection, cooling performance, water permeability and morphology was determined.
- The antimicrobial ability of the acrylic coating was assessed with regard to the impact of Ag-Zn/zeolite and 2-n-octyl-4-isothiazolin-3-one (OIT).

4. Layout of the thesis

The thesis comprises 119 pages, with 53 figures, 40 tables, and a bibliography of 114 references. The structure of the thesis follows a typical layout, which includes an introduction, three content chapters, and a conclusion. Notably, the novelty of the research has resulted in the publication of six papers, with four papers

listed in SCIE journals and two in Scopus-indexed journals, as well as a granted patent.

CHAPTER 1. OVERVIEW

Chapter 1 consists of 26 pages and includes 15 figures and 4 tables. This chapter provides an introduction to the current state of research and development in acrylic emulsion polymers, with a focus on enhancing their properties and applications. The chapter discusses a simple yet highly efficient approach, which involves incorporating metal oxide nanoparticles into acrylic emulsion polymers. However, due to differences in structure and nature, the dispersion of metal oxide nanoparticles in acrylic emulsion polymers remains a significant challenge. To address this, researchers often modify metal oxide nanoparticles using silane or titanate coupling agents to enhance their dispersion within the polymer matrix.

Chapter 1 also provides an overview of the current state of research and development in organic coatings that possess excellent solar reflection and antimicrobial properties. The overview reveals that multifunctional and environmentally friendly coatings, which include properties like solar reflection, high thermal stability, good weather resistance, good antimicrobial properties, and low volatile organic compounds, have not received as much attention with relatively low publication output. Previous work primarily focused on the individual effects of separate agents on coating properties. Solar-reflective and antibacterial coatings were traditionally prepared using separate agents, such as nanofillers or organic antibacterial additives. However, there has been a growing emphasis on the incorporation of both organic and inorganic additives. As a result, the study of the preparation and application of coatings based on acrylic emulsion polymers with nanofillers and antimicrobial additives has significantly expanded the possibilities for acrylic emulsion polymers. Furthermore, these coatings play a vital role in reducing cooling energy consumption and enhancing the aesthetics of buildings..

CHAPTER 2. EXPERIMENTAL

Chapter 2 is presented in 13 pages, 4 figures and 5 tables which includes:

2.1. Materials

2.2. Modified nanoparticles preparation

2.3. Acrylic nanocomposite coating preparation

2.4. Solar reflective coating preparation

2.5. Analysis

2.5.1. *Determination of characteristics, properties of modified nanoparticles*

The characteristics and properties of the modified nanoparticles were analyzed using various physical analytical instruments, available at the Vietnam Academy of Science and Technology and Vietnam National University, Hanoi. These instruments included FTIR, TGA, FESEM, XRD, DLS, and UV-Vis-NIR diffuse reflectance spectrometer.

2.5.2. *Determination of characteristics and properties of paint coating*

The properties of the paint coating, including abrasion resistance, water permeability, weather durability, resistance to microorganisms, and cooling performance, were determined in accordance with appropriate ASTM, ISO, and TCVN standards.

CHAPTER 3. RESULTS AND DISCUSSION

3.1. Study on modification of R-TiO₂ NPs and ZrO₂ NPs

3.1.1. *Characteristics and properties of organically modified R-TiO₂ NPs*

R-TiO₂ NPs were modified using two coupling agents, [3-(methacryloyloxy)propyl]trimethoxysilane (TMSPM) and isopropyl tri(dioctylpyrophosphate) titanate (KR-12), with an initial content of coupling agent at 3 wt% (relative to the weight of the NPs). These modified NPs are coded as mTi3T and mTi3K, respectively. The characteristics and properties of both native R-TiO₂ NPs (u-Ti) and the organically modified NPs were determined and are presented below.

3.1.1.1. *FTIR analysis*

As depicted in Figure 3.1, both the FTIR spectra of u-Ti and the modified NPs exhibit similar

characteristic absorptions located at 3438 and 1631 cm^{-1} (associated with O-H groups on the R-TiO₂ NPs' surface), as well as peaks at 1045 and 596 cm^{-1} (indicative of Ti-O linkages). The modified NPs' FTIR spectra reveal additional vibrations at 2925 cm^{-1} and 1383 cm^{-1} , attributed to C-H linkages (from KR12 and TMSPM). Notably, the FTIR spectrum of mTi3T shows a new peak at 945 cm^{-1} , corresponding to Ti-O-Si linkages. This indicates the successful organic modification of R-TiO₂ NPs.

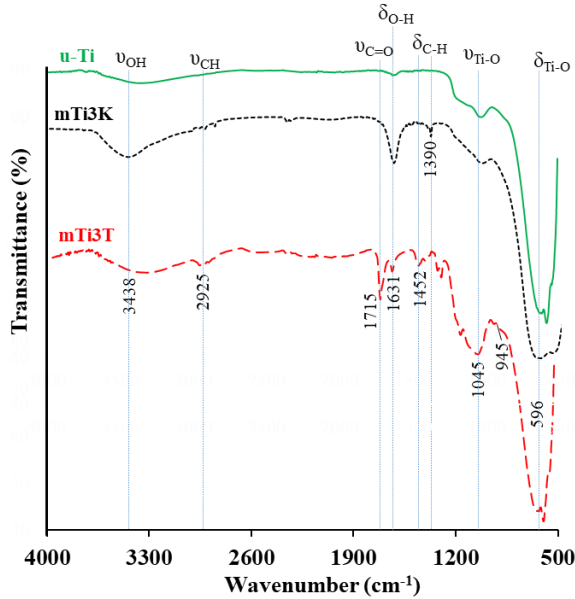


Figure 3.1. FTIR spectra of u-Ti, mTi3K and mTi3T

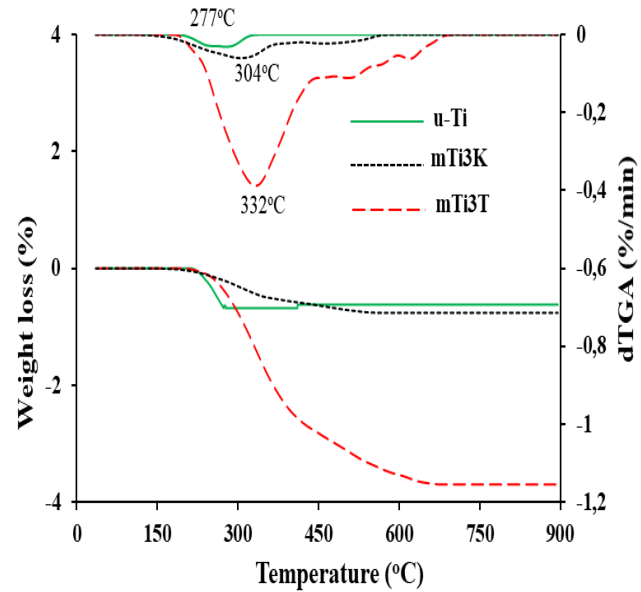


Figure 3.2. TGA and dTGA diagrams of u-Ti, mTi3K and mTi3T

3.1.1.2. Coupling agent content grafted on R-TiO₂ NPs

Table 3.1. Content of coupling agent grafted on R-TiO₂ NPs

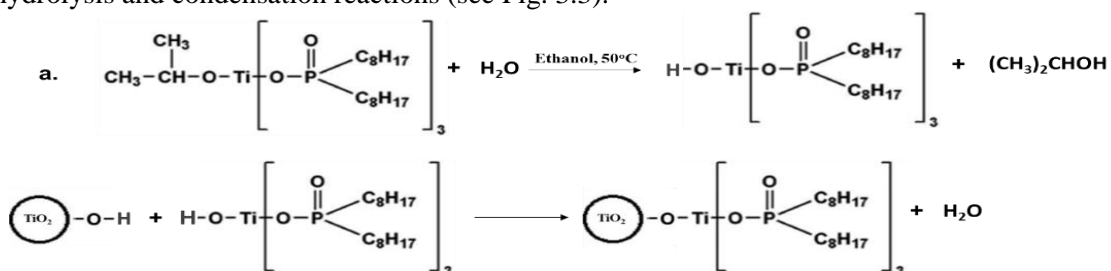
Sample	Weight loss at 900°C (%)	The maximum thermal degradation (°C)	Molecular weight of agent (au)	Content of agent grafted on NPs surface (mmol/g)
u-Ti	0.62	277	-	-
mTi3K	0.75	304	1311	10 ⁻³
mTi3T	3.7	322	248	0.122

On the base of Thermal Gravimetric Analysis (TGA) diagrams (Fig. 3.2), content of agent grafted on NPs surface can be calculated as follow formula:

$$\text{grafted content} \left(\frac{\text{mmol}}{\text{g}} \right) = \frac{\Delta m \cdot 10^3}{(100 - \Delta m) \cdot M_{\text{agent}}} \quad (1)$$

In there: Δm is weight loss of sample in temperature range of 100-900°C, M_{agent} is molecular weight of agent.

As can be seen from Table 3.1, although R-TiO₂ NPs were modified with the same initial content of TMSPM and KR12, the content of KR12 grafted onto the NPs is lower than that of TMSPM. The reason for this difference may be the variance in molecular weight and size of the functional groups, which can influence the hydrolysis and condensation reactions (see Fig. 3.3).



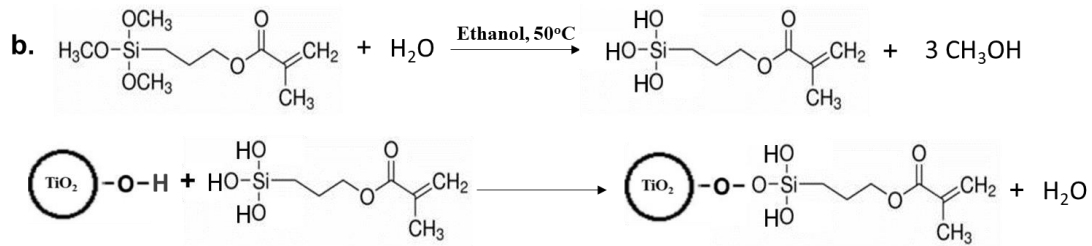


Figure 3.3. Mechanism of surface modification of R-TiO₂ with KR-12 (a)/TMSPM (b)

3.1.1.3. Morphology

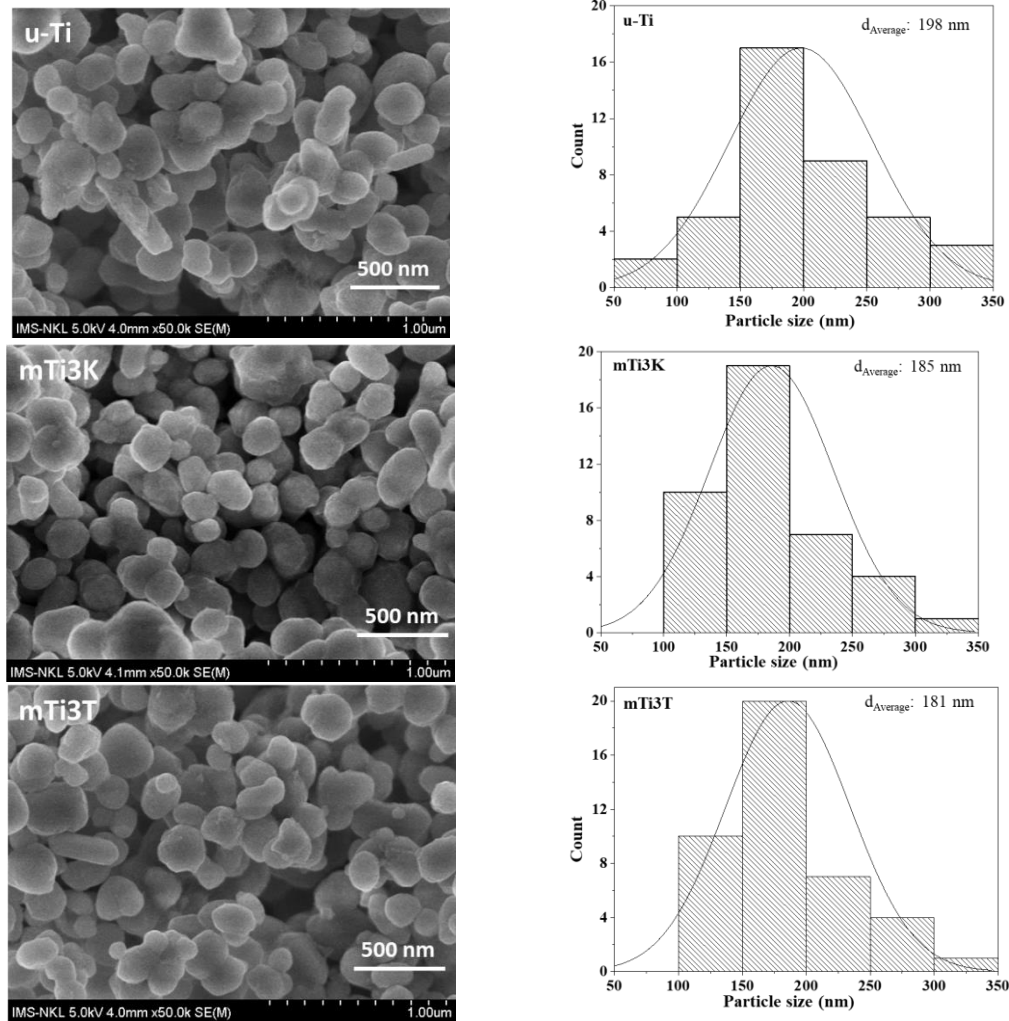


Figure 3.4. FESEM image and corresponding size distribution of u-Ti, mTi3T and mTi3K

As observed in Figure 3.4, there is an insignificant difference in the morphology of u-Ti and the modified R-TiO₂ NPs, namely mTi3T and mTi3K. Therefore, the organic surface modification has an insignificant influence on the morphology of R-TiO₂ NPs.

3.1.1.4. Size distribution analysis

Table 3.2. The average particle size of R-TiO₂ nanoparticles before and after organic modification when dispersed in water

No	Sample	Particle size range (nm)	Average particle size (nm)
1	u-Ti	615 - 1718	1032
2	mTi3K	342 - 1990	788
3	mTi3T	24 - 955	284

As depicted in Figure 3.5, the modified R-TiO₂ NPs exhibit better dispersion ability in water compared to u-Ti. The u-Ti NPs tend to agglomerate into larger clusters, with the particle size of u-Ti in water increasing

to six times its initial size. However, due to organic modification, the agglomeration of mTi3K and mTi3T is significantly reduced (refer to Table 3.2).

NPs possess high surface energy, which causes them to readily aggregate when dispersed in water as a means to reduce surface energy. Organic modification serves to reduce this surface energy and increase hydrophobicity. Despite the organic modification, FTIR spectrum analysis reveals (as discussed in Section 3.1.1.1) that both mTi3K and mTi3T still contain –OH groups, allowing the organically modified NPs to maintain good interaction with water. As a result, the size of the organically modified R-TiO₂ NPs is reduced when dispersed in water. Furthermore, mTi3T nanoparticles exhibit superior dispersion in water compared to mTi3K NPs due to a higher content of successfully grafted organic agents onto the surface of R-TiO₂ NPs (as discussed in Section 3.1.1.2). As a result, R-TiO₂ NPs modified with 3wt.% TMSPM (mTi3T) were selected for further studies.

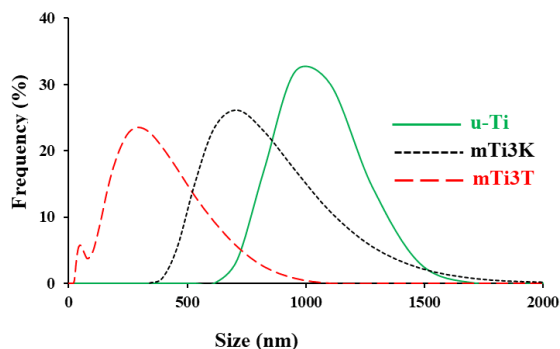


Figure 3.5. Size distribution diagrams of u-Ti, mTi3T and mTi3K

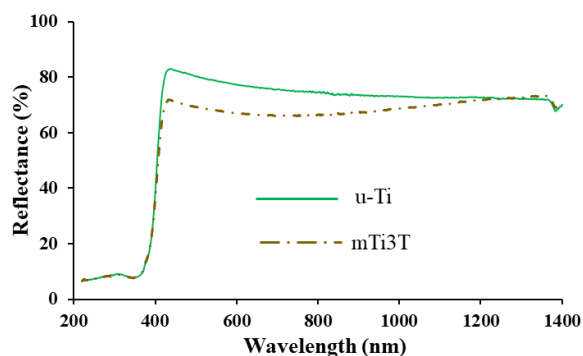


Figure 3.6. UV-Vis-NIR spectra of u-Ti and mTi3T

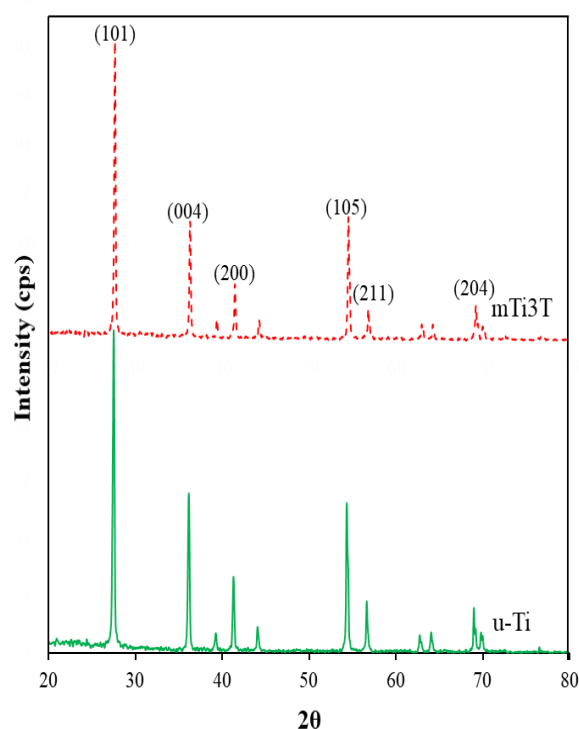


Figure 3.7. XRD patterns of u-Ti and mTi3T

3.1.1.5. UV-Vis-NIR diffuse reflectance spectroscopy analysis

The light reflection ability of mTi3T NPs is lower than that of u-Ti NPs, as illustrated in Fig. 3.6. This difference arises because the silane agents grafted onto the nanoparticle surface partially cover the nanoparticle surface area, thereby reducing the ability of the organically modified NPs to diffuse light reflection. It is worth noting that the NPs were modified with a relatively low content of silane coupling agent, only 3 wt.%. Consequently, the disparity in the light diffuse reflectance ability between u-Ti and mTi3T particles is not substantial.

3.1.1.6. XRD patterns analysis

No difference is observed between the XRD patterns of u-Ti and mTi3T NPs (see Fig. 3.7). This result demonstrates that the organic modification of the R-TiO₂ nanoparticle surface with the TMSPM agent does not alter the crystal structure of the R-TiO₂ NPs.

Thus, the characteristics and properties of organically modified R-TiO₂ NPs show that R-TiO₂ NPs modified with TMSPM have better dispersion and stability compared to those modified with KR12. Therefore, R-TiO₂ modified with TMSPM was chosen for further studies..

3.1.2. Characteristics and properties of organically modified ZrO₂ NPs

ZrO₂ NPs were modified using three coupling agents, [3-(methacryloyloxy)propyl]trimethoxysilane

(TMSPM), isopropyl tri(dioctylpyrophosphate) titanate (KR-12) and (3-glycidyoxypropyl)triethoxysilane (GPTES), with an initial content of coupling agent at 3 wt% (relative to the weight of the NPs). These modified NPs are coded as mZr3T, mZr3G và mZr3K, respectively. The characteristics and properties of both native ZrO₂ NPs (u-Zr) and the organically modified NPs were determined and are presented below.

3.1.2.1. FTIR analysis

Comparing the FTIR spectrum of u-Zr nanoparticles (Fig. 3.8) with that of organically modified ZrO₂, new absorption peaks at 2925 and 1402 cm⁻¹ are evident, which are characteristic of the C-H bond (CH₂ group) found in organic denaturing agents. Moreover, in the spectra of mZr3T and mZr3G, an additional absorption peak at 1048 cm⁻¹ is observed, characteristic of the Zr-O-Si bond. In the spectrum of mZr3K, an absorption peak at 1045 cm⁻¹ also emerges, characteristic of the deformation vibration of the Ti-O bond. These results serve as evidence that the ZrO₂ NPs were successfully modified by the organic agents.

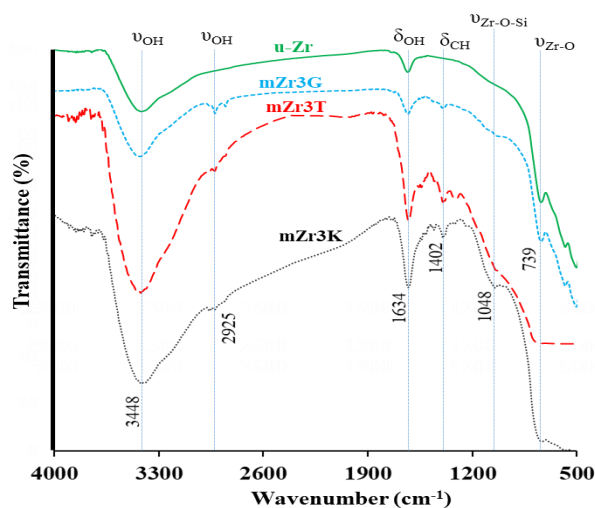


Figure 3.8. FTIR spectra of u-Zr, mZr3K, mZr3T and mZr3G

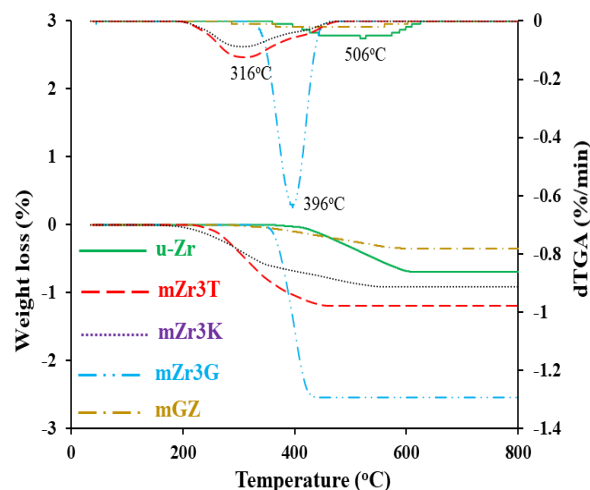


Figure 3.9. TGA and dTGA diagrams of u-Zr, mZr3K, mZr3T, mZr3G and mixture of hydrolyzed GPTES with ZrO₂ (mGZ)

3.1.2.2. Coupling agent content grafted on ZrO₂ NPs

It is evident that the thermogravimetric analysis curve of the mixture of hydrolyzed GPTES with ZrO₂ NPs (mGZ) shares a similar shape with that of u-Zr NPs, as shown in Fig. 3.9. Both mGZ and u-Zr exhibit mass loss within a temperature range of 400 to 600°C, with a peak decomposition temperature of 506°C. This observation affirms that, without heating, there is no dehydration reaction between the OH group of the silanol and the OH group on the nanoparticle surface. Furthermore, it indicates that the silanols that do not participate in the grafting reaction on the nanoparticle surface have been effectively removed.

By assessing the mass loss of ZrO₂ NPs before and after modification, the amount of grafting agent on the surface of ZrO₂ NPs can be calculated using the formula provided in Section 3.1.1.2 (refer to Table 3.3). It is evident that the content of GPTES agent grafted onto the nanoparticle surface is the highest, primarily due to the lower space density of the organic functional group in GPTES, as explained in Section 3.1.1.2.

Table 3.3. Content of coupling agent grafted on ZrO₂ NPs

Mẫu	Weight loss at 900°C (%)	The maximum thermal degradation (°C)	Molecular weight of agent (au)	Content of agent grafted on NPs surface (mmol/g)
u-Zr	0.69	506	-	-
mZr3K	0.91	308	1311	1.6.10 ⁻³
mZr3T	1.19	316	248	0.02
mZr3G	2.54	396	278	0.068

3.1.2.3. Morphology

The FESEM image (Fig. 3.10) illustrates that after organic modification, the size of ZrO₂ NPs does not

change significantly and remains the same as that of u-Zr NPs. Therefore, the surface organic modification process does not alter the size of ZrO₂ NPs.

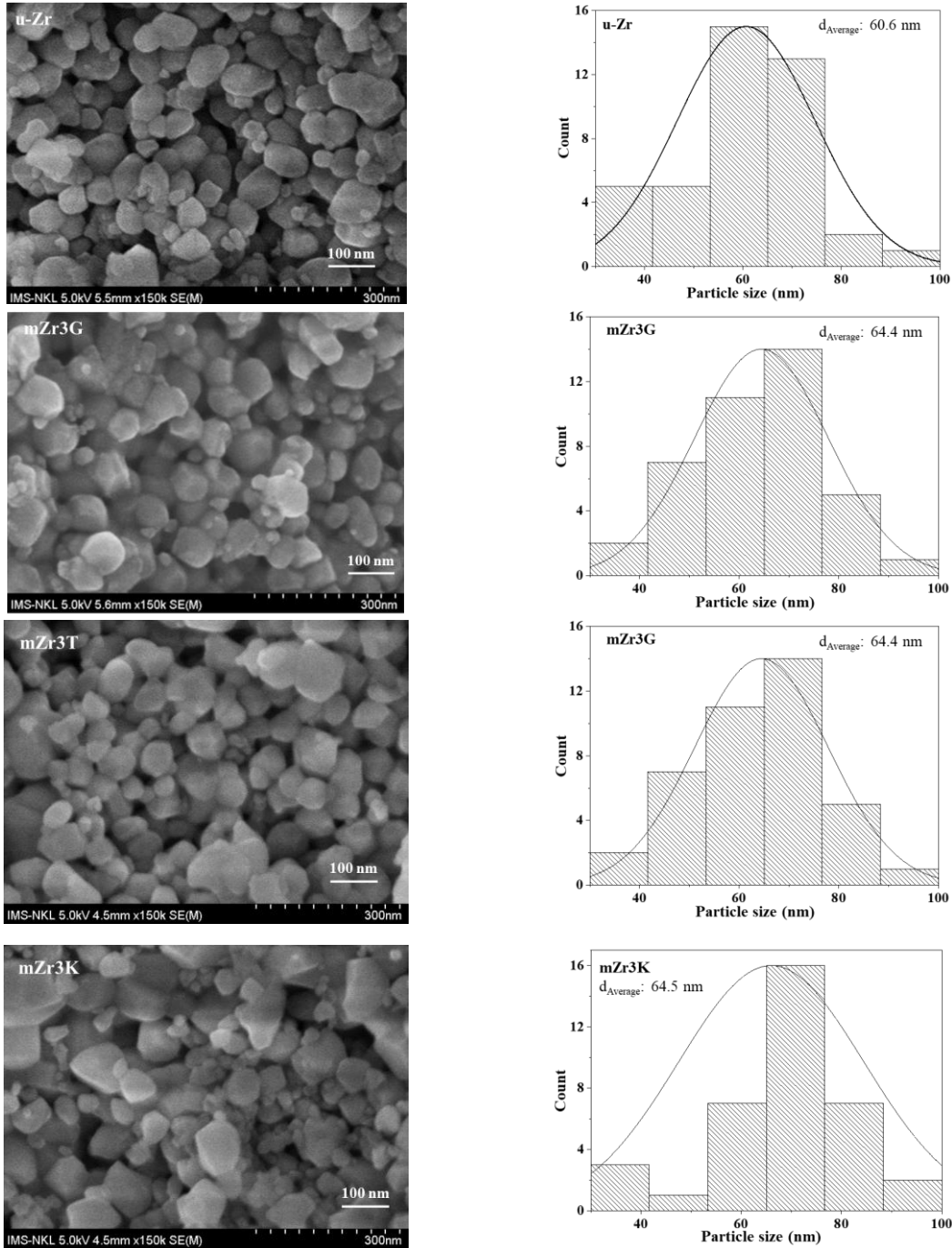


Figure 3.10. FESEM images and corresponding size distribution of u-Zr, mZr3T, mZr3K and mZr3G

3.1.2.4. Size distribution analysis

Table 3.4. The average particle size of ZrO₂ nanoparticles before and after organic modification when dispersed in water

No	Sample	Particle size range (nm)	Average particle size (nm)
1	u-Zr	193 - 655	345
2	mZr3K	171 - 513	313
3	mZr3T	171 - 655	301
4	mZr3G	134 - 585	255

It is evident that when dispersed in water, organically modified ZrO_2 NPs exhibit better dispersibility and greater stability compared to u-Zr NPs, as illustrated in Fig. 3.11. Notably, mZr3G NPs demonstrate the highest dispersibility in water, with the smallest average dispersed particle size (refer to Table 3.4).

As a result, ZrO_2 NPs modified with GPTES exhibit superior stability in water when compared to ZrO_2 NPs modified with other agents. Consequently, GPTES-modified ZrO_2 NPs have been selected for further studies.

3.1.2.5. UV-Vis-NIR diffuse reflectance spectroscopy analysis

It can be observed that the diffuse reflection of light from mZr3G NPs is lower than that from u-Zr NPs (see Fig. 3.12). However, the difference in diffuse reflection of light between u-Zr and mZr3G NPs is not consistent.

3.1.2.6. XRD patterns analysis

Comparing the XRD patterns of u-Zr and mZr3G NPs, as shown in Fig. 3.13, reveals that there is no difference between the two XRD patterns of u-Zr and mZr3G NPs.

Thus, the results of the research on the organic modification of the surface of ZrO_2 NPs with coupling agents KR12, TMSPM, GPTES demonstrate that, with the same content of denaturing agent (3wt.% in comparison to NPs), the amount of GPTES grafted onto the surface of ZrO_2 NPs is the highest. Consequently, mZr3G NPs exhibit stability and superior properties. Therefore, ZrO_2 NPs organically modified with GPTES have been selected for further studies.

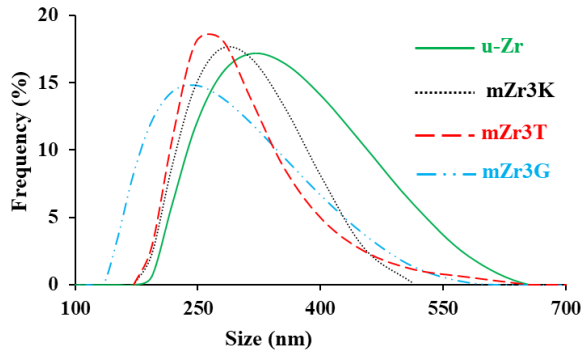


Figure 3.11. Size distribution diagrams of u-Zr, mZr3T, mZr3K and mZr3G

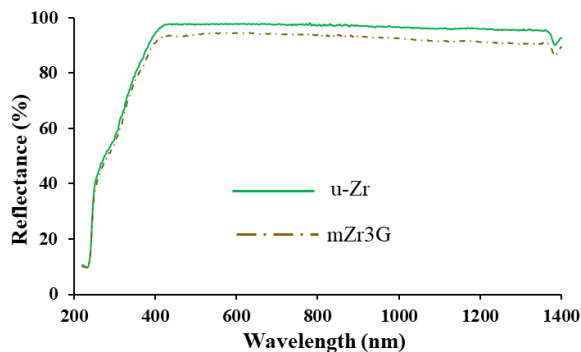


Figure 3.12. UV-Vis-NIR spectra u-Zr and mZr3G

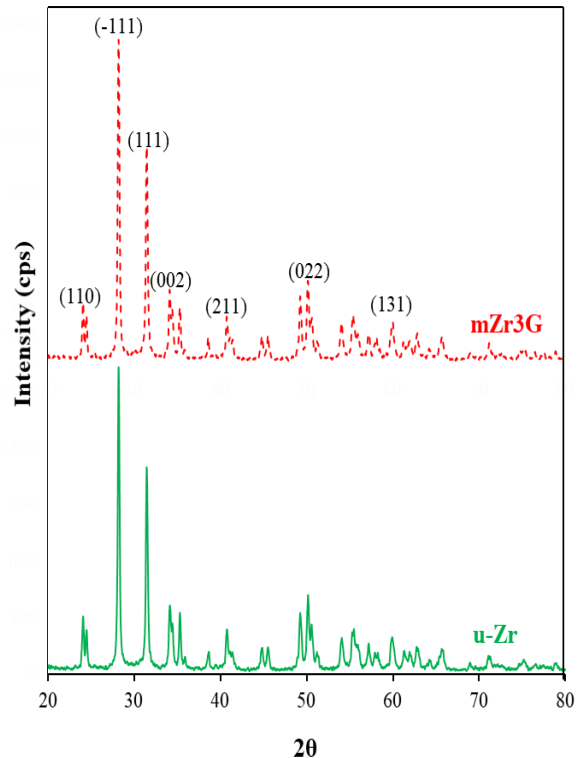


Figure 3.13. XRD patterns of u-Zr and mZr3G

3.2. Characteristics and properties of acrylic coating filled with R-TiO₂ và ZrO₂ NPs

3.2.1. Effect of organically modified R-TiO₂ NPs on acrylic coating's properties

The properties of nanocomposite coatings largely depend on the dispersion ability and metal oxide nanoparticle content. As a result, it is crucial to determine the suitable content of organically modified metal oxide NPs in the paint film, as well as the appropriate content of the organic agent for modifying metal oxide NPs. In this study, the falling abrasion resistance test was employed to determine the optimal modifier content and the appropriate content of organically modified NPs.

3.2.1.1. Effect of coupling agent content

The study aimed to determine the effect of TMSPM agent content used for modifying R-TiO₂ NPs (referred

to as mTi_xT, where x = 1, 3, 5, 10, and 20wt.% TMSPM compared to R-TiO₂ NPs) on the falling abrasion resistance of acrylic coating containing 2wt.% R-TiO₂ NPs (refer to Table 3.5). The differences in falling abrasion resistance among the investigated coatings were determined through ANOVA statistical analysis, complemented by posthoc Tukey HSD analysis (see Table 3.6).

Table 3.5. Abrasion resistance of acrylic coating with various nanofillers.

Sample	Abrasion resistance (L/mil)	ANOVA oneway
A0	84 ± 3.35	<i>F</i> : 287.8
AuT	135 ± 3.83	<i>P</i> _{value} : 8.1.10 ⁻²⁴
A2mTi1T	174 ± 4.24	
A2mTi3T	187 ± 6.62	
A2mTi5T	142 ± 3.25	
A2mTi10T	128 ± 2.33	
A2mTi20T	125 ± 2.86	

Table 3.6. Post-Hoc Tukey HSD results for the difference in abrasion resistance of acrylic coatings with various nanofillers

Sample pair	Tukey HSD Q statistic	Tukey HSD p value	Tukey HSD inference
A0 vs AuT	25.6	0.001	p < 0.05
A0 vs A2mTi1T	45.1	0.001	p < 0.05
A0 vs A2mTi3T	51.6	0.001	p < 0.05
A0 vs A2mTi5T	29.1	0.001	p < 0.05
A0 vs A2mTi10T	22.2	0.001	p < 0.05
A0 vs A2mTi20T	20.6	0.001	p < 0.05
AuT vs A2mTi1T	19.4	0.001	p < 0.05
AuT vs A2mTi3T	25.9	0.001	p < 0.05
AuT vs A2mTi5T	3.4	0.223	Insignificant
AuT vs A2mTi10T	3.5	0.202	Insignificant
AuT vs A2mTi20T	5.0	0.020	p < 0.05
A2mTi1T vs A2mTi3T	6.5	0.001	p < 0.05
A2mTi1T vs A2mTi5T	15.9	0.001	p < 0.05
A2mTi1T vs A2mTi10T	22.9	0.001	p < 0.05
A2mTi1T vs A2mTi20T	24.4	0.001	p < 0.05
A2mTi3T vs A2mTi5T	22.5	0.001	p < 0.05
A2mTi3T vs A2mTi10T	29.4	0.001	p < 0.05
A2mTi3T vs A2mTi20T	30.9	0.001	p < 0.05
A2mTi5T vs A2mTi10T	6.9	0.001	p < 0.05
A2mTi5T vs A2mTi20T	8.5	0.001	p < 0.05
A2mTi10T vs A2mTi20T	1.5	0.899	Insignificant

The results indicate that the acrylic film containing unmodified R-TiO₂ NPs (AuT) exhibits 1.6 times higher abrasion resistance than the neat acrylic coating (A0). This improvement can be attributed to the high hardness of R-TiO₂ NPs, which, when combined with the coating, enhances the coating's hardness and abrasion resistance. Additionally, the small size of R-TiO₂ NPs allows them to fill in defects within the coating, creating a denser structure and enhancing mechanical properties, such as drop abrasion resistance. However, inorganic NPs often have poor dispersion within organic polymer matrix and may not fully exploit their properties. Organic surface modification enhances the compatibility of nano R-TiO₂ with polyacrylic. Therefore, the abrasion resistance of A2mTi1T and A2mTi3T coatings surpasses that of AuT coating. However, when the TMSPM content exceeds 5 wt %, abrasion resistance decreases. It is possible that with an increase in TMSPM content, an organic layer forms on the surface of R-TiO₂ NPs, and TMSPM polymerizes to create a new phase

within the coating structure. This may introduce defects and reduce abrasion resistance. As a result, the acrylic coating containing mTi3T NPs is chosen for further studies

3.2.1.2. Effect of mTi3T content on properties of acrylic coating

The impact of mTi3T content on the abrasion resistance of acrylic coating (symbolized as AxmTi3T, with x = 0.5, 1, 2, and 4 wt % mTi3T) has been assessed (refer to Table 3.7). Differences between the coatings were determined through ANOVA statistical analysis, complemented by post-hoc Tukey HSD analysis (see Table 3.8).

Table 3.7. Abrasion resistance of acrylic coating with various mTi3T content

Sample	Abrasion resistance (L/mil)	ANOVA oneway
A0.5mTi3T	158 ± 2.88	$F = 23.1$ $p_{value} = 4.6 \cdot 10^{-24}$
A1mTi3T	173 ± 5.08	
A2mTi3T	187 ± 6.62	
A4mTi3T	173 ± 4.46	

The results indicated that an increase in the content of mTi3T NPs led to improved abrasion resistance. However, when the content increased to 4 wt.%, abrasion resistance begins to decline. The A2mTi3T coating exhibits the highest abrasion resistance, reaching 187 L/mil. This enhancement is attributed to the organically modified R-TiO₂ NPs, which improve dispersion, fill defects, and reinforce the acrylic coating, thus enhancing abrasion resistance. Nevertheless, increasing the content to 4 wt.% can lead to nanoparticle agglomeration, which in turn reduces sand abrasion resistance. Consequently, the A2mTi3T coating has been selected for further research.

Table 3.8. Post-Hoc Tukey HSD results for the difference in abrasion resistance of acrylic coatings with various mTi3T content

Sample pair	Tukey HSD Q statistic	Tukey HSD p value	Tukey HSD inference
A0.5mTi3T vs A1mTi3T	6.1	0.002	p < 0.05
A0.5mTi3T vs A2mTi3T	11.8	0.001	p < 0.05
A0.5mTi3T vs A4mTi3T	6.2	0.002	p < 0.05
A1mTi3T vs A2mTi3T	5.7	0.004	p < 0.05
A1mTi3T vs A4mTi3T	0.1	0.899	Insignificant
A2mTi3T vs A4mTi3T	5.6	0.005	p < 0.05

3.2.1.3. Morphology of acrylic coating filled with R-TiO₂ NPs

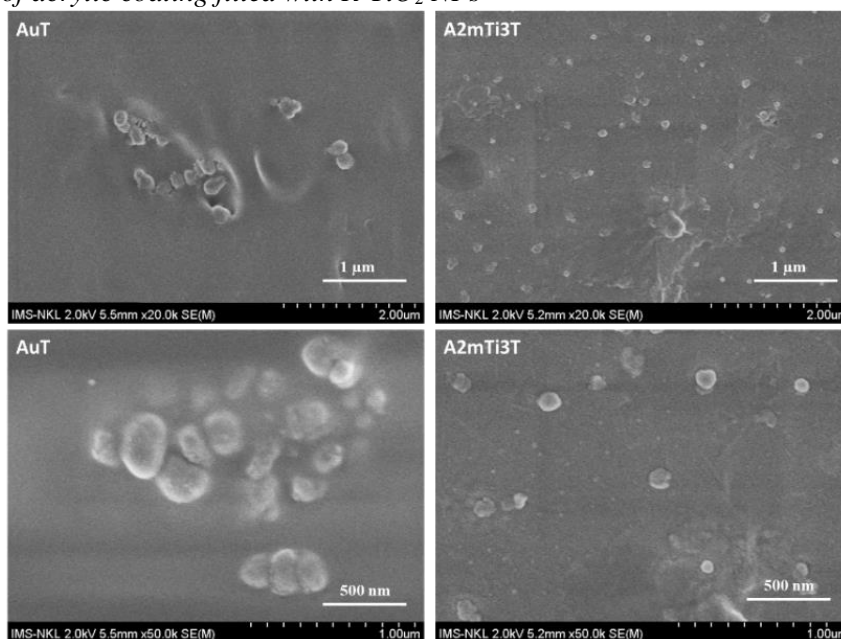


Figure 3.14. FESEM images of AuT and A2mTi3T

The FESEM images (Fig. 3.14) illustrate that the AuT coating features u-Ti NPs agglomerated, forming larger-sized particles. In contrast, after organic modification, the R-TiO₂ NPs are uniformly dispersed in the coating, with R-TiO₂ NPs size of approximately 100 nm and less agglomeration compared to the AuT coating.

In comparison with u-Ti, mTi3T exhibits the ability to disperse effectively in acrylic emulsion polymer, thereby enhancing the mechanical properties of the acrylic coating. Consequently, the A2mTi3T coating has been selected for further studies.

3.2.2. Effect of organically modified ZrO₂ NPs on acrylic coating's properties

3.2.2.1. Effect of coupling agent content

The study aims to assess the effect of the content of the GPTES agent used for modifying ZrO₂ NPs (referred to as mZrxG, where x = 1, 3, 5, 10, and 20 wt% GPTES compared to ZrO₂ NPs) on the abrasion resistance of acrylic films containing 2 wt % ZrO₂ NPs (refer to Table 3.9). Differences between the coatings were determined through ANOVA statistical analysis, supplemented by post-hoc Tukey HSD analysis (see Table 3.10).

Table 3.9. Abrasion resistance of acrylic coating with various nanofillers

Sample	Abrasion resistance (L/mil)	ANOVA oneway
A0	84 ± 3.35	F = 316, p _{value} = 2.2.10 ⁻²⁴
AuZ	77 ± 2.64	
A2mZr1G	156 ± 3.4	
A2mZr3G	174 ± 3.6	
A2mZr5G	155 ± 7.1	
A2mZr10G	151 ± 5.7	
A2mZr20G	150 ± 6.9	

Table 3.10. Post-Hoc Tukey HSD results for the difference in abrasion resistance of acrylic coatings with various nanofillers

Sample pair	Tukey HSD Q statistic	Tukey HSD p value	Tukey HSD inference
A0 vs AuZ	2.8	0.466	Insignificant
A0 vs A2mZr1G	33.0	0.001	p < 0.05
A0 vs A2mZr3G	41.0	0.001	p < 0.05
A0 vs A2mZr5G	32.4	0.001	p < 0.05
A0 vs A2mZr10G	30.7	0.001	p < 0.05
A0 vs A2mZr20G	34.9	0.001	p < 0.05
AuZ vs A2mZr1G	35.7	0.001	p < 0.05
AuZ vs A2mZr3G	43.7	0.001	p < 0.05
AuZ vs A2mZr5G	35.1	0.001	p < 0.05
AuZ vs A2mZr10G	33.5	0.001	p < 0.05
AuZ vs A2mZr20G	37.6	0.001	p < 0.05
A2mZr1G vs A2mZr3G	8.0	0.001	p < 0.05
A2mZr1G vs A2mZr5G	0.6	0.899	Insignificant
A2mZr1G vs A2mZr10G	2.2	0.661	Insignificant
A2mZr1G vs A2mZr20G	1.8	0.804	Insignificant
A2mZr3G vs A2mZr5G	8.6	0.001	p < 0.05
A2mZr3G vs A2mZr10G	10.2	0.001	p < 0.05
A2mZr3G vs A2mZr20G	6.1	0.003	p < 0.05
A2mZr5G vs A2mZr10G	1.6	0.899	Insignificant
A2mZr5G vs A2mZr20G	2.5	0.566	Insignificant
A2mZr10G vs A2mZr20G	4.1	0.083	Insignificant

The results indicate that the abrasion resistance of the film containing unmodified ZrO₂ NPs (AuZ) is not

significantly different from that of the A0 coating due to poor dispersion of ZrO_2 particles. After organic modification, ZrO_2 NPs achieve better dispersion, resulting in increased sand falling abrasion resistance. The coating containing mZr3G NPs exhibits the highest durability and has been selected for further research.

3.2.2.2. Effect of mZr3G content on properties of acrylic coating

The study aims to investigate the impact of mZr3G content on the abrasion resistance of acrylic coatings (symbolized as AxmZr3G, with x = 0.5, 1, 2, 3, and 5 wt % mZr3G). The differences between the coatings were determined through ANOVA statistical analysis, complemented by post-hoc Tukey HSD analysis (see Table 3.12).

Table 3.11. Abrasion resistance of acrylic coating with various mZr3G content

Sample	Abrasion resistance (L/mil)	ANOVA oneway
A0.5mZr3G	142 ± 4.92	F = 24, p _{value} = 1.66.10 ⁻⁷
A1mZr3G	152 ± 5.69	
A2mZr3G	174 ± 3.6	
A3mZr3G	172 ± 7.52	
A5mZr3G	156 ± 6.9	

The results indicate that with an increase in mZr3G content, the abrasion resistance of the coating rises. However, when the mZr3G content exceeds 2 wt %, the increase in abrasion resistance becomes gradual and eventually decreases. The acrylic film containing 2 wt % of mZr3G NPs exhibited the highest durability, reaching 174 L/mil, and has been selected for further research.

Table 3.12. Post-Hoc Tukey HSD results for the difference in abrasion resistance of acrylic coatings with various mZr3G content

Sample pair	Tukey HSD Q statistic	Tukey HSD p value	Tukey HSD inference
A0.5mZr3G vs A1mZr3G	3.5	0.126	Insignificant
A0.5mZr3G vs A2mZr3G	11.2	0.001	p < 0.05
A0.5mZr3G vs A3mZr3G	10.5	0.001	p < 0.05
A0.5mZr3G vs A5mZr3G	4.8	0.021	p < 0.05
A1mZr3G vs A2mZr3G	7.7	0.001	p < 0.05
A1mZr3G vs A3mZr3G	7.0	0.001	p < 0.05
A1mZr3G vs A5mZr3G	1.2	0.898	Insignificant
A2mZr3G vs A3mZr3G	0.6	0.899	Insignificant
A2mZr3G vs A5mZr3G	6.4	0.001	p < 0.05
A3mZr3G vs A5mZr3G	5.7	0.004	p < 0.05

3.2.2.3. Morphology of acrylic coating filled with ZrO_2 NPs

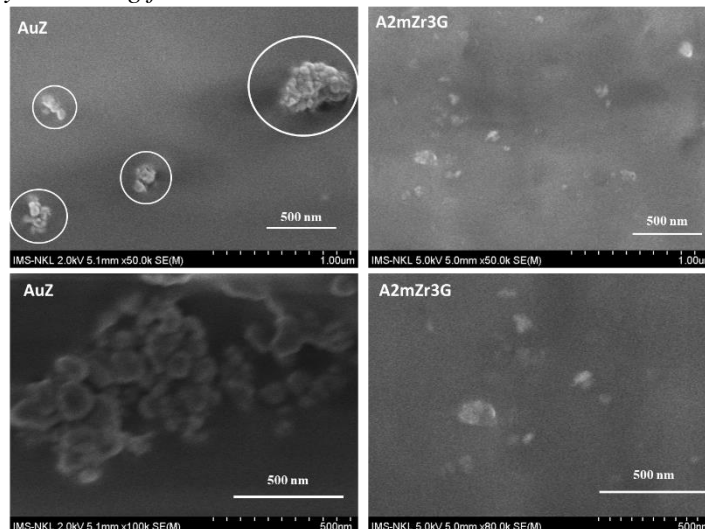


Figure 3.15. FESEM images of AuZ, A2mZr3G

The FESEM images (Figure 3.14) illustrate that the AuZ coating contains u-Zr NPs that agglomerate to form larger particles. However, the mZr3G NPs disperse quite evenly within the acrylic coating and the agglomeration of mZr3G NPs is significantly reduced. This is the reason why the abrasion resistance of the film containing mZr3G NPs is significantly greater than that of the acrylic coating without NPs

In comparison to u-Zr nanoparticles, ZrO₂ NPs modified with 3wt% GPTES (mZr3G) exhibit a superior ability to disperse within the acrylic polymer matrix, thereby enhancing the abrasion resistance of the coating. This paint has been chosen for further studies.

3.2.3. Effect of mZr3G NPs and mTi3T NPs on acrylic coating's properties

3.2.3.1. Effect of mZr3G NPs and mTi3T NPs on acrylic coating's abrasion resistance

The study examines the impact of the mTi3T/mZr3G ratio (specifically, mTi3T/mZr3G = 2/0, 1.5/0.5, 1/1, 0.5/1.5, and 0/2) on the abrasion resistance of acrylic coating (refer to Table 3.13). Differences between the coatings were determined through ANOVA statistical analysis, complemented by post-hoc Tukey HSD analysis (see Table 3.14). The coating that combines two types of NPs exhibits higher abrasion resistance than the coating containing each type of nanoparticle separately. The difference in particle size (mTi3T NPs: 160 nm, mZr3G NPs: 60 nm) may be a contributing factor. The smaller size of these modified NPs allows them to better fill defects and micro-holes in the coating, increasing uniformity and continuity. Therefore, the A1TZ and A15TZ coatings have been selected for further research

Table 3.13. Abrasion resistance of acrylic coating filled with various weight ratio of mZr3G and mTi3T

Sample	Abrasion resistance (L/mil)	ANOVA oneway
A2mT	187 ± 6.62	F = 18,03 p _{value} = 10 ⁻⁴
A15TZ	188 ± 3.33	
A1TZ	199 ± 3.78	
AT15Z	181 ± 3.14	
A2mZ	172 ± 7.52	

Table 3.14. Post-Hoc Tukey HSD results for the difference in abrasion resistance of acrylic coatings filled with various weight ratio of mZr3G and mTi3T

Sample pair	Tukey HSD Q statistic	Tukey HSD p value	Tukey HSD inference
A2mT vs A15TZ	2.479	0.449	Insignificant
A2mT vs A1TZ	6.970	0.0042	p < 0.01
A2mT vs AT15Z	0.793	0.8999	Insignificant
A2mT vs A2mZ	4.495	0.0596	Insignificant
A15TZ vs A1TZ	4.491	0.0598	Insignificant
A15TZ vs AT15Z	3.272	0.2174	Insignificant
A15TZ vs A2mZ	6.974	0.0041	p < 0.01
A1TZ vs AT15Z	7.763	0.0019	p < 0.01
A1TZ vs A2mZ	11.465	0.0010	p < 0.01
AT15Z vs A2mZ	3.701	0.1399	Insignificant

3.2.3.2. Effect of mZr3G and mTi3T NPs on acrylic coating's light diffuse reflectance

The diffuse reflectance spectra of acrylic films containing different weight ratios of mZr3G/mTi3T exhibit noticeable differences (see Figure 3.16). Interestingly, the difference in coating thickness is negligible (refer to Table 3.15). The coating that contains both mTi3T and mZr3G NPs concurrently demonstrates superior light diffusion reflection efficiency compared to the coating containing only one type of nanoparticle. This enhancement is attributed to the resonance effect and interaction between R-TiO₂ and ZrO₂ NPs when combined. The A1TZ coating exhibits the highest light reflection ability and has been selected for further research.

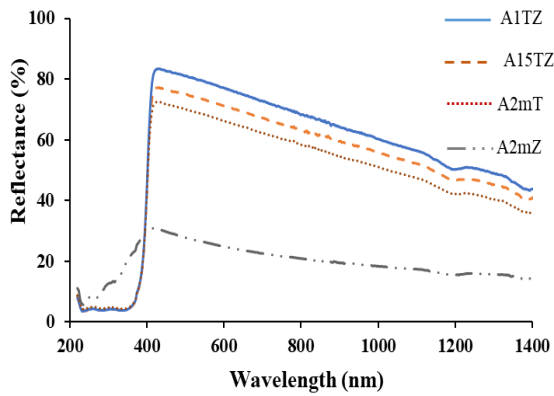


Figure 3.16. UV-Vis-NIR spectra of acrylic coatings filled with various weight ratio of mZr3G and mTi3T

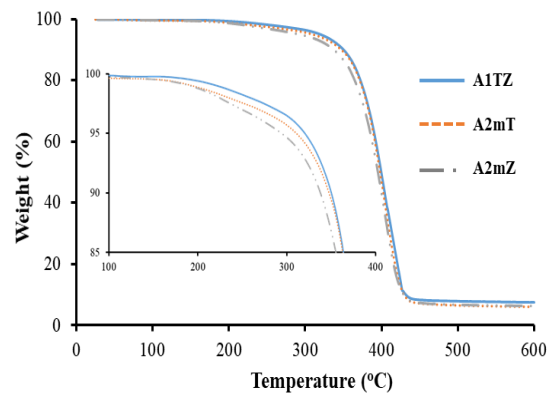


Figure 3.17. TGA diagrams of acrylic coatings filled with various weight ratio of mZr3G and mTi3T

Table 3.15. The average thickness and reflection index of acrylic coatings filled with various weight ratio of mZr3G and mTi3T

Sample	Average thickness (μm)	Reflection index (400-1400 nm), (%)
A2mT	59.4 ± 0.29	54.45
A15TZ	59.1 ± 0.43	59.41
A1TZ	57.2 ± 0.34	64.12
A2mZ	58.1 ± 0.79	20.65

3.2.3.3. Effect of mZr3G and mTi3T NPs on acrylic coating's thermal stability

The TGA diagram (Figure 3.17) reveals that the A1TZ coating has the highest starting weight loss temperature and thermal stability when compared to the other coatings. This effect can be attributed to the interaction and insertion of mTi3T and mZr3G NPs into defects and micropores within the coating, coupled with the smaller size of mZr3G NPs in comparison to mTi3T NPs. This interaction leads to a tighter, uniform, and continuous structure of the coating, which restricts the adverse effects of high temperatures and the penetration of oxygen into the coating.

3.2.3.4. Effect of mZr3G and mTi3T NPs on acrylic coating's weather durability

Accelerated weather testing, also known as artificial weather testing, is an effective method for rapidly predicting the lifespan or durability of polymer coatings. The extent of deterioration or aging in acrylic films can be assessed by monitoring changes in functional group content, primarily through FTIR spectroscopy, and measuring weight loss during the accelerated weather testing.

- FTIR spectroscopy analysis

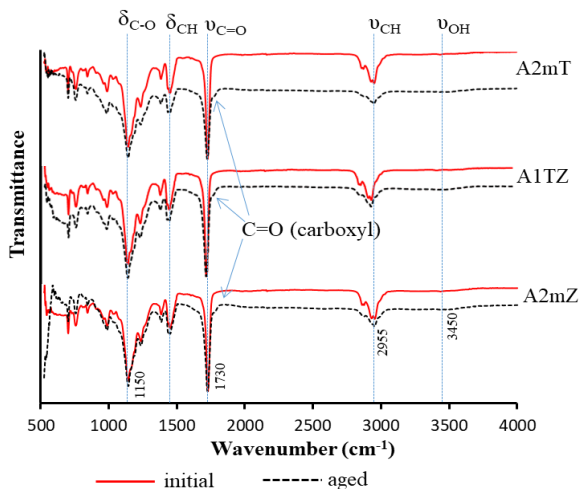


Figure 3.18. FTIR spectra of acrylic coatings filled with different weight ratios of mZr3G and mTi3T at both the initial stage and after 54 aging cycles

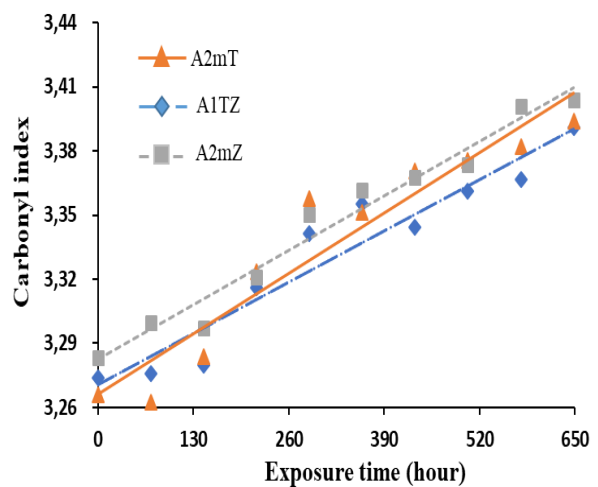


Figure 3.19. The change of CI of acrylic coatings filled with different weight ratios of mZr3G and mTi3T upon weathering test

FTIR spectrum analysis (Figure 3.18) reveals that the coating, following the accelerated weathering test, displays a new absorption peak at 1780 cm^{-1} , a characteristic of the valence vibration of the C=O bond in the carboxylic acid group. Furthermore, in comparison to the FTIR spectrum of the coating before the accelerated weathering test, alterations in the intensity of absorption peaks have been observed. Specifically, the intensity of the absorption peak at 3440 cm^{-1} , characteristic of the O-H bond, has increased, while the intensity of the absorption peaks related to the C=O, C-H, and C-O bonds has decreased.

In assessing the weather resistance of coatings during accelerated weather testing, the carbonyl group index (CI) and photooxidation index (PI) are commonly employed. These indices are calculated based on the intensity of spectral peaks associated with the carbonyl group (1730 cm^{-1}) and the OH group (3450 cm^{-1}) in comparison to the intensity of the C-H group (1450 cm^{-1}). Throughout the course of accelerated weather testing, both the CI index (Figure 3.18) and the PI index (Figure 3.19) for acrylic coatings exhibit only minor increases. This suggests that acrylic coatings containing organically modified nanoparticles demonstrate robust weather resistance.

Table 3.16. The slope of the trend lines indicating the variation in the carbonyl index and photooxidation index of acrylic coating filled with different weight ratios of mZr3G and mTi3T upon weathering test

Sample	The slope of the trend lines of carbonyl index ($\times 10^{-4}$)	The slope of the trend lines of photooxidation index ($\times 10^{-5}$)
A1TZ	1.85	8.33
A2mT	2.18	9.54
A2mZ	1.96	8.54

However, it's important to note that the slopes of the trend lines representing the changes in the CI and PI indices of the coatings differ. Notably, the slope of the trend lines for the CI and PI indices in the A1TZ paint film is the lowest (as indicated in Table 3.16). This signifies that the A1TZ paint film exhibits the highest level of weather resistance among the surveyed acrylic coatings.

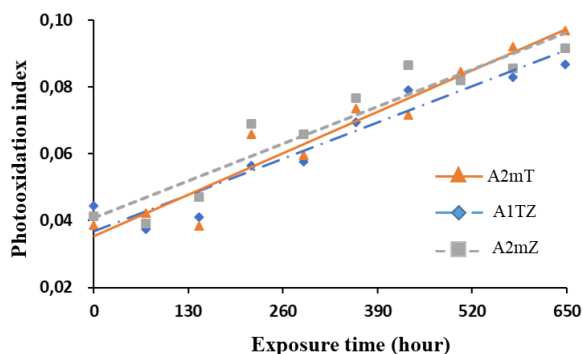


Figure 3.20. The change of photooxidation index of acrylic coatings filled with different weight ratios of mZr3G and mTi3T upon weathering test

- *Weight loss of acrylic coatings upon weathering test*

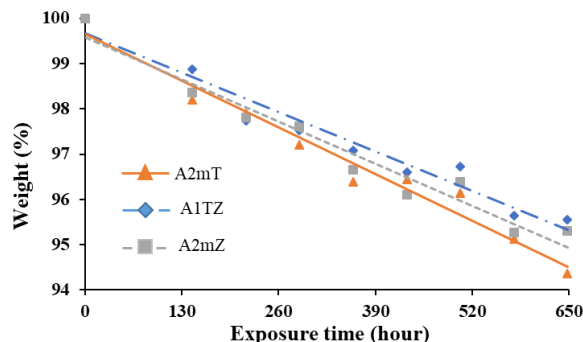


Figure 3.21. The change of weight loss of acrylic coatings filled with different weight ratios of mZr3G and mTi3T upon weathering test

It is evident that the change in weight loss of the coatings during the accelerated weathering test is relatively small (as shown in Figure 3.21). Even after 54 testing cycles, the weight of the coating has only decreased by approximately 5%. This outcome reaffirms the high weather durability of the investigated acrylic coatings. Notably, the slope of the trend line for mass loss in the A1TZ coating is the lowest, indicating that the A1TZ coating boasts the most exceptional weather durability.

Thus, combining mTi3T and mZr3G NPs can create a synergistic effect enhancing the properties of acrylic coatings (sand abrasion resistance, thermal durability, light diffuse reflection and weather resistance) compared to a coating containing only one specific type of nanoparticle.

3.3. Study on improvement of solar reflective coating properties

3.3.1. Effect of nanoparticles on acrylic coating's solar reflection

Based on the results obtained in section 3.2, the mixture of mTi3T + mZr3G NPs (with a weight ratio of 1/1) was selected for use as an additive in solar reflective paint (SRP) on the base of acrylic emulsion polymer.

The effect of the mixture of mTi3T + mZr3G NPs content replacing R-TiO₂ micro particles on the solar reflective paint formula was determined using the diffuse reflectance spectrum of coatings, namely SRP, SRP0.5, SRP1 and SRP2. These coatings have a composition corresponding to the content of the mTi3T + mZr3G nanoparticle mixture used to replace R-TiO₂ microparticles, which are 0%, 0.5%, 1% and 2%, respectively. Details of this change can be observed based on the diffuse reflectance spectrum of the coatings (Figure 3.22) as well as the thickness and diffuse reflectance of the paint films (Table 3.18). It can be seen that replacing micro R-TiO₂ particles with a mixture of mTi3T + mZr3G NPs has contributed to increasing the diffuse reflection light ability of the paint film to reflect solar heat. One of the reasons may be because the mTi3T + mZr3G nanocomposite has a very small size and good compatibility with the polyacrylic substrate. This allows them to fill in the gaps and micro-holes between R-TiO₂ microparticles in the structure of the paint film to reflect solar heat. Thanks to that, the ability to diffuse reflection light of the solar thermal reflective paint film containing the mTi3T + mZr3G nanoparticle mixture has been significantly improved (Figure 3.23). SRP1 paint film with good reflectivity will be selected for further research.

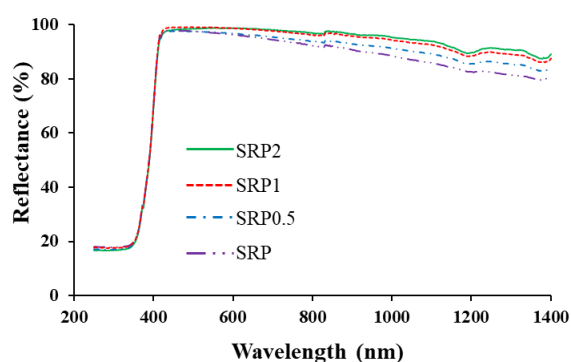


Figure 3.22. Diffuse reflectance spectra of SRP and paint filled with various content of mixture mTi3T + mZr3G replacing R-TiO₂ microparticles

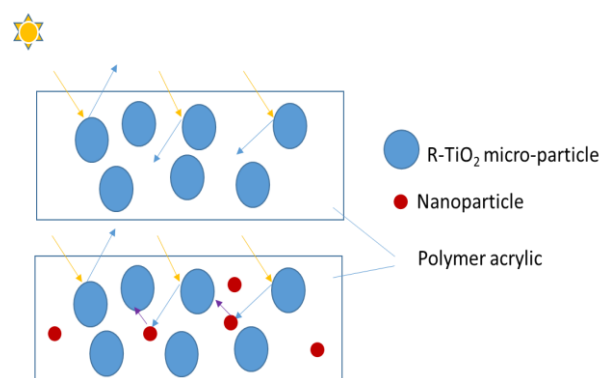


Figure 3.23. The structure simulates a solar heat-reflecting paint film without and with a mixture of organically modified inorganic nanoparticles

Table 3.17. The average thickness and reflection index of of SRP and paint filled with various content of mixture mTi3T + mZr3G replacing R-TiO₂ microparticles

Sample	Average thickness (μm)	Reflection index (400-1400 nm), (%)
SRP	100.9 ± 1.34	89.77
SRP0.5	100.1 ± 1.51	91.80
SRP1	99.7 ± 1.44	94.46
SRP2	101.8 ± 1.59	94.89

3.3.2. Cooling performance of solar reflective paint

Cooling performance of the solar reflective paint system containing the mTi3T + mZr3G nanoparticle mixture (SRP1) and the comparison to the waterproof paint system (based on acrylic resin combined with cement) has been determined. Changes in the surface temperature of the test chamber and the air temperature in the test chamber of the paint systems are presented in Figure 3.24 - Figure 3.26, respectively. It can be seen that when replacing 1% of R-TiO₂ microparticles, it increased the cooling performance.

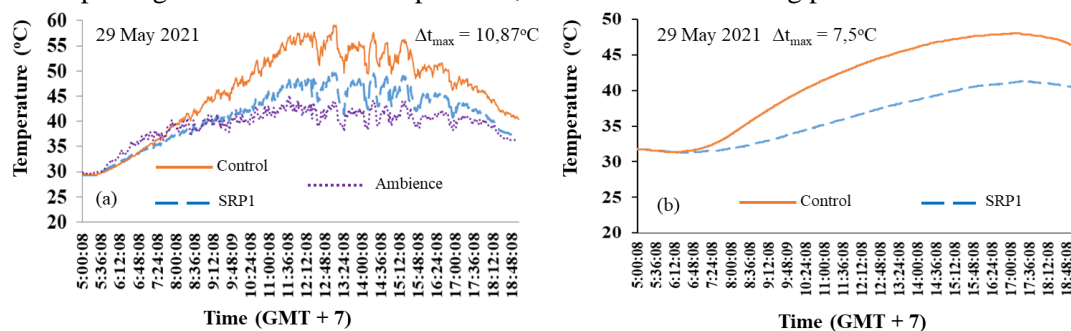


Figure 3.24. Difference in outside surface temperature (a) and air temperature (b) in the test chamber coated with SRP1 paint compared to the control chamber

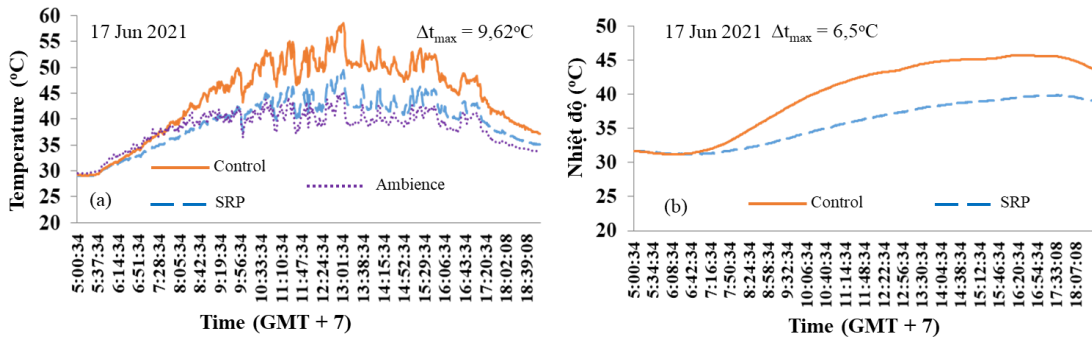


Figure 3.25. Difference in outside surface temperature (a) and air temperature (b) in the test chamber coated with SRP paint compared to the control chamber

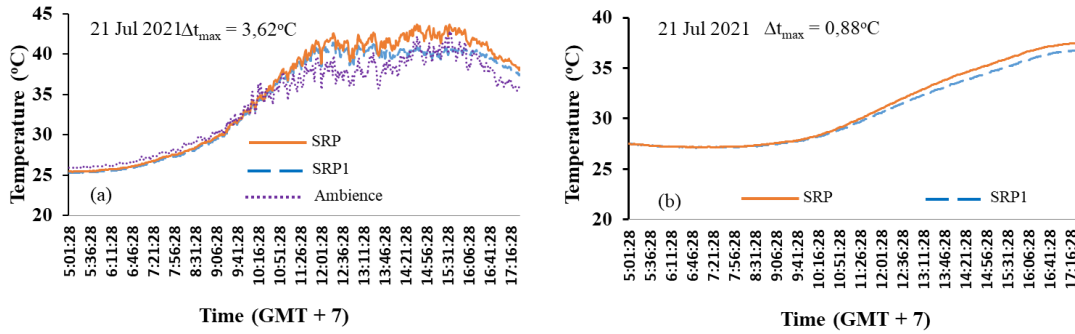


Figure 3.26. Difference in outside surface temperature (a) and air temperature (b) in the test chamber coated with SRP1 paint compared to the test chamber coated with SRP paint

3.3.3. Water permeability

It is evident that the water permeability of the SRP1 paint film is significantly lower than that of the SRP paint film (Table 3.18). This indicates that the paint film containing the mTi3T + mZr3G nanoparticle mixture exhibits higher water resistance compared to the paint film without the modified nanoparticle mixture.

Table 3.18. Water permeability of SRP and SRP1

Sample	Water permeability (g. m ⁻² h ^{-0.5})
SRP	0.0113 ± 0.0005
SRP1	0.0058 ± 0.0004

3.3.4. Morphology of solar reflective paint

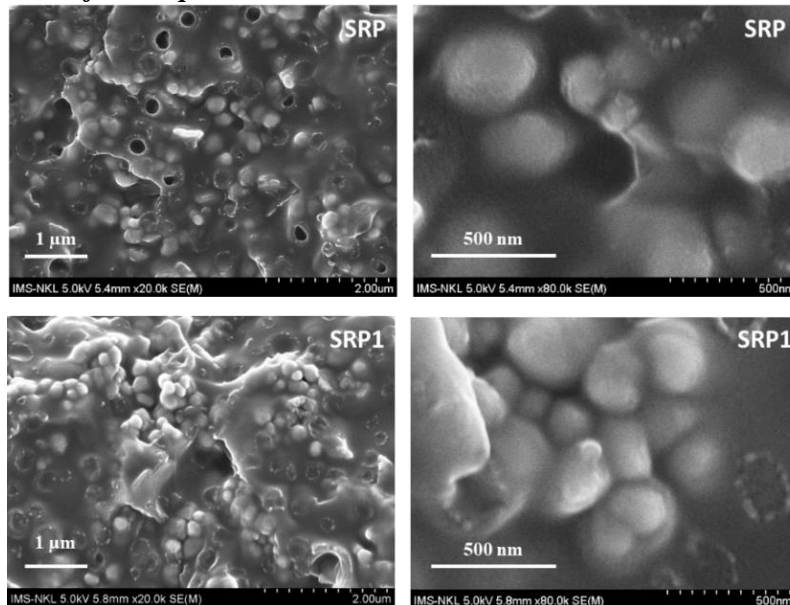


Figure 3.27. FESEM images of cross section of SRP and SRP1

The FESEM images show (Figure 3.27) that the SRP paint film is not uniform, with many defects such as gaps and micro-pores. For the SRP1 paint film, containing organically modified nanoparticles mTi3T + mZr3G, the paint film structure is tighter and uniform. The micropores are smaller in size and the paint film has fewer defects than the SRP paint film. This is the reason why the properties of SRP1 paint film are better than SRP.

Therefore, the substitution of R-TiO₂ microparticles with organically modified nanoparticles (mTi3T + mZr3G) in the solar reflective paint formulation has resulted in improvements in various properties of the paint film, including its light diffusion and reflectivity, heat resistance, and water resistance.

3.4. Study on improvement of acrylic coatings' microbial ability

To enhance the longevity of organic coatings, it is crucial to address the influence of microorganisms. Effective antimicrobial properties are essential to extend the shelf life of coatings. In typical paint formulations, R-TiO₂ granules are commonly employed as pigments, known for their excellent coverage capabilities. Notably, the addition of nano-sized R-TiO₂ particles in small quantities can significantly enhance various paint film properties, including mechanical properties, heat resistance, solar reflectivity, and weather durability. Given the multifaceted factors affecting paint film performance, we will focus our research on antimicrobial additives within an acrylic paint formulation that includes 2 wt % of mTi3T (A2mT) particles.

3.4.1. Effect of Ag-Zn/zeolite on acrylic coatings properties

3.4.1.1. Effect of Ag-Zn/zeolite on acrylic coatings abrasion resistance

The abrasion resistance of acrylic coating containing 1 wt % Ag-zn/zeolite (AZe) is nearly 2 times higher than that of neat acrylic coating (A0) (84 L/mil), but smaller than A2mT coating (Table 3.19). When adding Ag-Zn/zeolite agent to A2mT coating with a content of 0.5; 1 and 2 wt % (denoted as AmT0.5Ze, AmT1Ze and AmT2Ze, respectively) reduced the abrasion resistance of the coating. The results of ANOVA statistical analysis and post-hoc Tukey HSD analysis showed significant results regarding abrasion resistance between these coatings (Table 3.20). It proves that Ag-Zn/zeolite does not greatly affect the mechanical properties of the coating.

Table 3.19. Abrasion resistance of acrylic coating filled with 2 wt % mTi3T incorporation with various Ag-Zn/zeolite content

Sample	Abrasion resistance (L/mil)	ANOVA oneway
AZe	166 ± 3.84	$F = 12.4$ $p_{value} = 2.9 \cdot 10^{-5}$
A2mT	187 ± 6.62	
AmT0.5Ze	179 ± 3.77	
AmT1Ze	175 ± 4.34	
AmT2Ze	169 ± 3.64	

Table 3.20. Post-hoc Tukey HSD results of abrasion resistance of acrylic coating filled with 2 wt % mTi3T incorporation with various Ag-Zn/zeolite content

Sample pair	Tukey HSD Q statistic	Tukey HSD p value	Tukey HSD inference
AZe vs A2mT	8.8	0.001	p < 0.05
AZe vs AmT0.5Ze	5.4	0.008	p < 0.05
AZe vs AmT1Ze	3.9	0.079	Insignificant
AZe vs AmT2Ze	1.1	0.899	Insignificant
A2mT vs AmT0.5Ze	3.4	0.148	Insignificant
A2mT vs AmT1Ze	4.9	0.017	p < 0.05
A2mT vs AmT2Ze	7.7	0.001	p < 0.05
AmT0.5Ze vs AmT1Ze	1.5	0.802	Insignificant
AmT0.5Ze vs AmT2Ze	4.3	0.042	p < 0.05
AmT1Ze vs AmT2Ze	2.8	0.295	Insignificant

3.4.1.2. Effect of Ag-Zn/zeolite on acrylic coating antimicrobial ability

Table 3.21. Antibacterial activity of acrylic coatings filled with 2 wt % mTi3T incorporation with various Ag-Zn/zeolite content for *E. Coli* strain

Result of bacteria array			Antibacterial activity R	Dead bacteria (%)
Incubation time	0 h	24 h		
Samples	Log (average CFU/cm ²)	Log (average CFU/cm ²)		
Control	4.00 ± 0.04	4.03 ± 0.05	-	-
A2mT	4.00 ± 0.04	4.03 ± 0.05	< 0.1	0
AmT0.5Ze	4.00 ± 0.04	1.52 ± 0.05	2.51 ± 0.1	99.69
AmT1Ze	4.00 ± 0.04	0.04	3.99±0.05	99.99
AmT2Ze	4.00 ± 0.04	0.04	3.99±0.05	99.99

Table 3.22. Antibacterial activity of acrylic coatings filled with 2 wt % mTi3T incorporation with various Ag-Zn/zeolite content for *S. aureus* strain

Result of bacteria array			Antibacterial activity R	Dead bacteria (%)
Incubation time	0 h	24 h		
Samples	Log (average CFU/cm ²)	Log (average CFU/cm ²)		
Control	4,08	4,01 ± 0,05	-	-
A2mT	4,08	4,00 ± 0,05	< 0,1	2,28
AmT0.5Ze	4,08	1,72 ± 0,03	2,29 ± 0,08	99,49
AmT1Ze	4,08	0,38 ± 0,01	3,63 ± 0,06	99,98
AmT2Ze	4,08	0,04 ± 0,01	3,97 ± 0,06	99,99

The addition of Ag-Zn/zeolite to the coating significantly enhances its antibacterial properties, effectively eliminating 99% of *E. coli* (Table 3.21) and *S. aureus* (Table 3.22) bacteria. As the content of Ag-Zn/zeolite additive increases, the bactericidal effectiveness of the coating also increases. However, there is no discernible difference between the AmT1Ze and AmT2Ze coatings. Therefore, the AmT1Ze coating has been chosen for further investigation

3.4.1.3. Effect of Ag-Zn/zeolite on thermal stability of acrylic coating

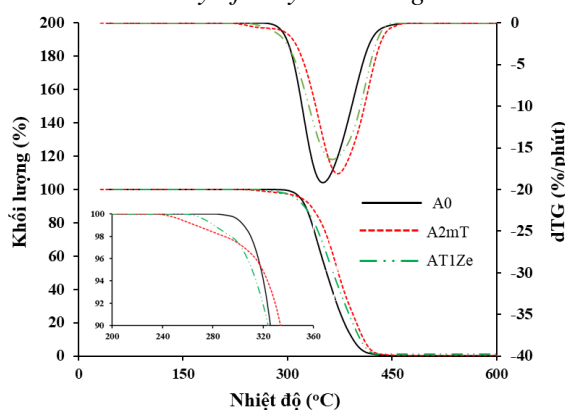


Figure 3.28. TGA and dTGA of acrylic coating filled with various fillers

Table 3.23. TGA parameters of acrylic coating filled with mTi3T and Ag-Zn/zeolite

Sample	T _{onset} (°C)	T _{offset} (°C)	T _{max} (°C)
A0	321	391	350
A2mT	338	406	372
AT1Ze	324	404	364

The TGA analysis (Figure 3.28 and Table 3.23) indicates that coatings with added Ag-Zn/zeolite agents exhibit lower thermal stability compared to acrylic coating containing solely organically modified nano R-TiO₂.

3.4.1.4. Effect of Ag-Zn/zeolite on weather resistance of acrylic coating

- FTIR spectroscopy analysis

Based on the FTIR spectrum analysis of the coating before and after weather testing (Figure 3.29) and an analysis of changes in the intensity of spectral features (Table 3.24), alterations in the carbonyl index (CI) (Figure 3.30) and the photooxidation index (PI) (Figure 3.31) of the coatings have been determined. It was observed that the A0 coating tended to exhibit the largest increase in the CI index but the smallest increase in the PI index.

Table 3.24. Changes in the characteristic absorption of functional groups in acrylic coatings containing mTi3T NPs and Ag-Zn/zeolite before and after accelerated weathering tests

Absorption (cm ⁻¹)	Characteristics	Before	After	Observation
3440	Stretching of O-H linkage	+	+	Increase
2925	Stretching of C-H linkage	+	+	Decrease
1780	Stretching of C=O linkage (of acid group)	-	+	Appearance
1730	Stretching of C=O linkage (Carbonyl group)	+	+	Not clearly
1450	Vibration deformation of C-H linkage	+	+	Decrease
1150	Vibration deformation of C-O linkage	+	+	Decrease

Note: “+” absorption; “-” No absorption

Based on FTIR spectrum analysis of the coating before and after weather testing (Figure 3.29) and the analysis of changes in the intensity of spectral fringes (Table 3.24), the changes in the carbonyl index (CI) (Figure 3.30) and the photooxidation index (PI) (Figure 3.31) of the acrylic coatings have been determined. It was found that the A0 coating tended to have the largest increase in the CI index but the smallest increase in the PI.

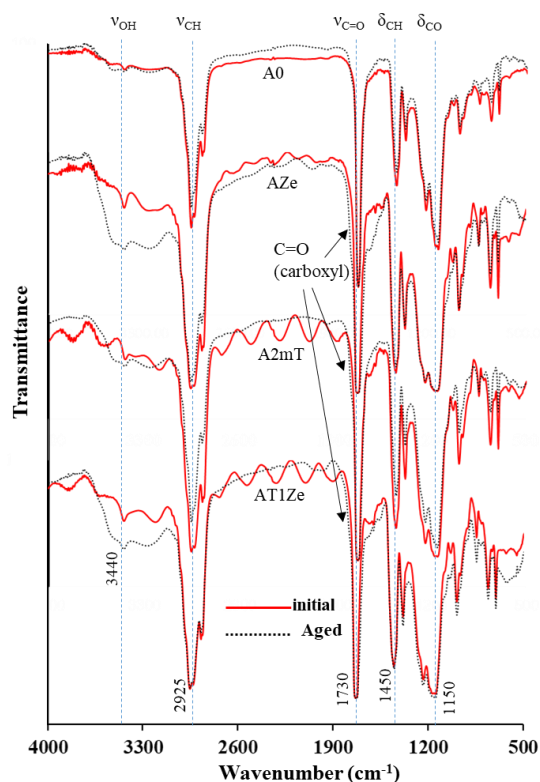


Figure 3.30. FTIR of acrylic coating filled with mTi3T and Ag-Zn/zeolite before and after (36 chu kỳ - 432 giờ) weathering test

- Weight loss of acrylic coating filled with mTi3T NPs and Ag-Zn/zeolite

During testing, the weight of acrylic coatings containing additives tended to increase during the first 72 hours of accelerated weathering test (Figure 3.32). After that, the weight of these coatings tends to decrease. The

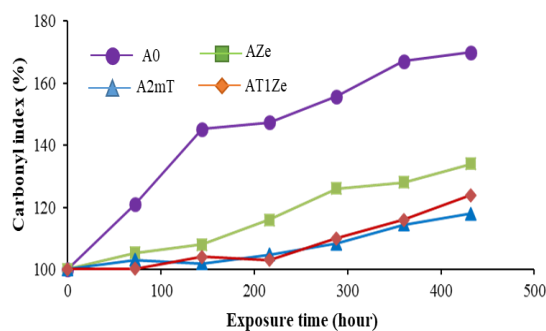


Figure 3.29. The CI changes of acrylic coating filled with mTi3T and Ag-Zn/zeolite before and after (36 chu kỳ - 432 giờ) weathering test.

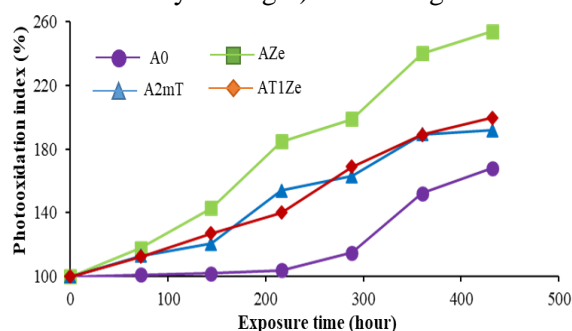


Figure 3.31. The PI changes of acrylic coating filled with mTi3T and Ag-Zn/zeolite before and after (36 chu kỳ - 432 giờ) weathering test

reason for this difference is that the degradation mechanisms of acrylic coatings containing and without different additives are different (Figure 3.32 and Figure 3.33)..

Thus, Ag-Zn/zeolite additive does not enhance the properties of acrylic coating (falling sand abrasion resistance, thermal resistance and weather resistance) like mTi3T NPs. However, acrylic coatings containing Ag-Zn/zeolite have good antibacterial properties. Acrylic coating containing 1% wt Ag-Zn/zeolite is capable of killing 99% of *E. coli* and *S. aureus* bacteria after 24 hours of testing.

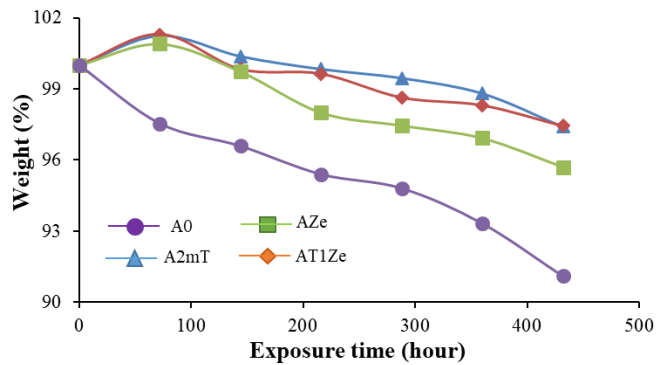


Figure 3.32. The change of weight acrylic coating filled with mTi3T NPs and Ag-Zn/zeolite upon weathering test

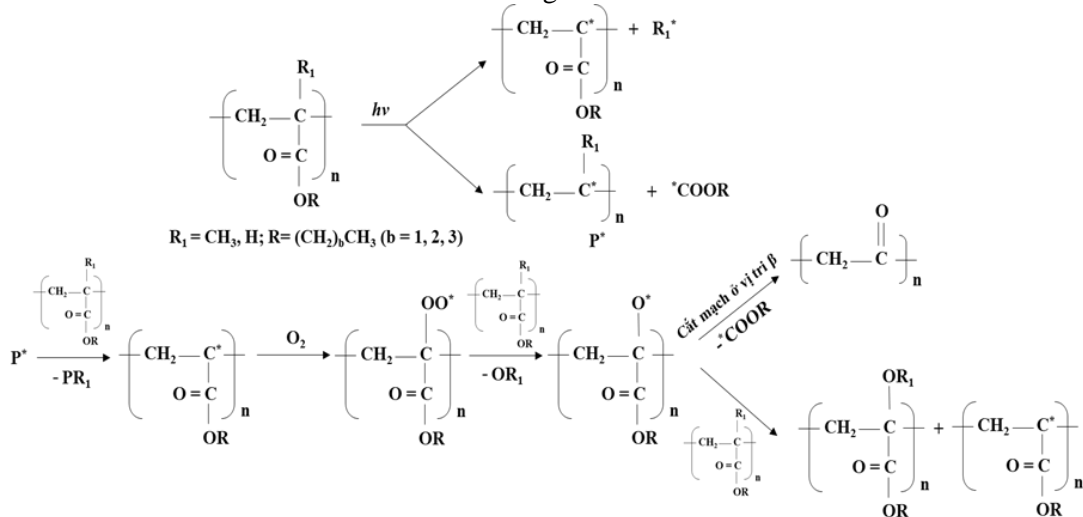


Figure 3.33. Assuming the photochemical degradation reaction mechanism of neat acrylic coating during accelerated weather testing

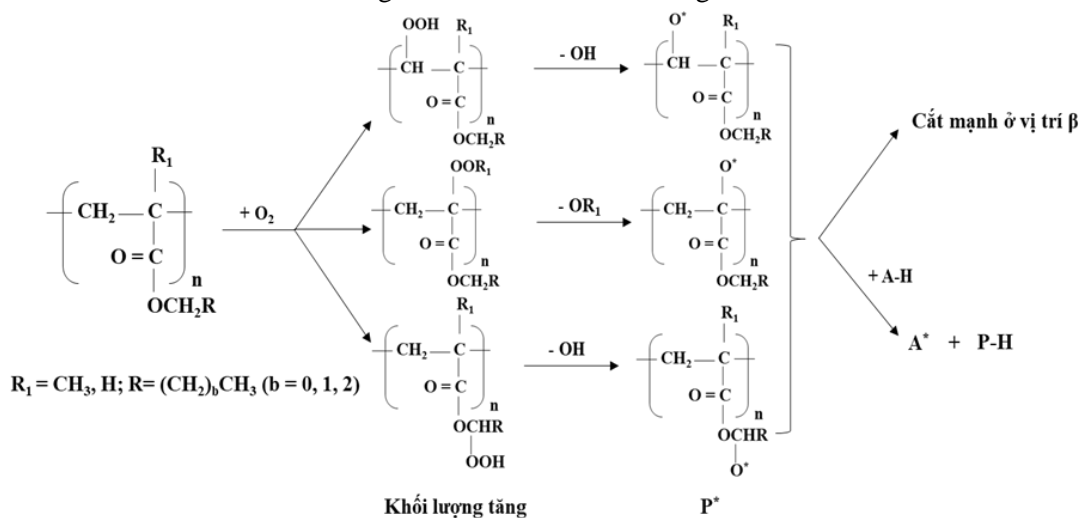


Figure 3.34. Hypothesized mechanism of activating oxygen molecules to attack polyacrylic circuits, leading to weight loss of acrylic coating containing additives during accelerated weather testing

3.4.2. Study on acrylic coating filled with OIT

3.4.2.1. Effect of OIT content on antibacterial ability

2-Octyl-4-isothiazolin-3-one (OIT) can inhibit the growth of microorganisms at very small concentrations (minimum inhibitory concentration (MIC) of OIT in the range of 2.5-10 parts per million (ppm)). Therefore, in this project, the OIT content is very small at 0.1%, 0.2% and 0.5% to investigate the anti-microbial ability of A2mT acrylic coating without investigating the effect of the content. OIT affects the mechanical properties (abrasion resistance) and thermal stability of the acrylic coating. Test results show that OIT has no antibacterial activity against two strains of bacteria *E. coli* (Table 3.25) and *S. aureus* (Table 3.26).

Table 3.25. Antibacterial activity of acrylic coatings filled with various OIT content for *E. Coli* strain

Result of bacteria array			Antibacterial activity R	Dead bacteria (%)
Incubation time	0 h	24 h		
Sample	Log (Average CFU/cm ²)	Log (Average CFU/cm ²)		
Control	4.00 ± 0.04	4.03	-	-
A2mT/0.1 %kl OIT	4.00 ± 0.04	4.03	< 0.1	0
A2mT/0.2 %kl OIT	4.00 ± 0.04	4.03	< 0.1	0
A2mT/0.5 %kl OIT	4.00 ± 0.04	4.03	< 0.1	0

Table 3.26. Antibacterial activity of acrylic coatings filled with various OIT content for *S. aureus* strain

Result of bacteria array			Antibacterial activity R	Dead bacteria (%)
Incubation time	0 h	24 h		
Sample	Log (Average CFU/cm ²)	Log (Average CFU/cm ²)		
Mẫu đối chứng	4.08 ± 0.04	4.01 ± 0.05	-	-
A2mT/0.1 %kl OIT	4.08 ± 0.04	4.01 ± 0.05	< 0.1	0
A2mT/0.2 %kl OIT	4.08 ± 0.04	4.01 ± 0.05	< 0.1	0
A2mT/0.5 %kl OIT	4.08 ± 0.04	4.01 ± 0.05	< 0.1	0

3.4.2.2. Effect of OIT and Ag-Zn/zeolite on mold of acrylic coating

Table 3.27. Antifungal ability of acrylic coating contains different OIT content and 1 wt % Ag-Zn/zeolite

Sample	Evaluation time (day)	Percentage of surface area contaminated with fungi (%)	Antifungal level
A2mT/0.1 %kl OIT	28	0	1
A2mT/0.2 %kl OIT	28	0	0
A2mT/0.5 %kl OIT	28	0	0
AT1Ze	28	11	2b
AT1Ze/0.1 %kl OIT	28	0	0

Acrylic coating containing organically modified R-TiO₂ NPs combined with OIT is not capable of killing *E. coli* and *S. aureus* bacteria with an OIT content of 0.1 - 0.5 wt %. However, this acrylic coating has good antifungal properties. Acrylic coating using a combination of 1 wt % Ag-Zn/zeolite and 0.1 wt % OIT has the ability to synergistically enhance antibacterial and antifungal activity.

3.4.3. Effect of agents on antimicrobial ability of solar reflective paint

3.4.3.1. Effect of agents on light diffuse reflectance

From the results obtained in sections 3.4.1 and 3.4.2, the additive mixture Ag-Zn/zeolite and OIT was selected as an anti-microbial additive for the solar reflective paint (SRPK) formulation. It can be seen that SRPK's ability to reflect light is not different from SRP1.

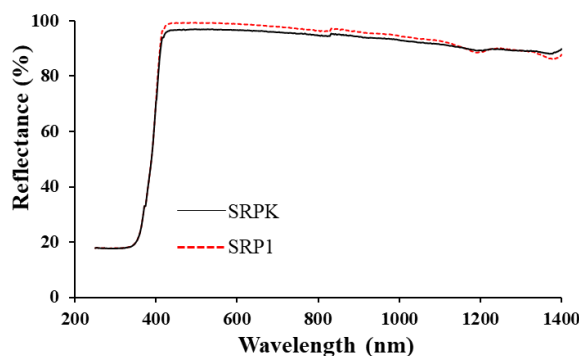


Figure 3.35. Diffuse reflectance spectroscopy of solar reflective paint with different antibacterial agents

3.4.3.2. The antibacterial ability of solar reflective paint contains different antimicrobial additives

Table 3.28. Antibacterial activity of solar reflective paint filled with various antimicrobial agents for *E. coli* strain

Result of bacteria array			Antibacterial activity R	Dead bacteria (%)
Incubation time	0 h	24 h		
Sample	Log (Average CFU/cm ²)	Log (Average CFU/cm ²)		
Control	4.04 ± 0.04	4.06 ± 0.05	-	-
SRP1	4.04 ± 0.04	1.35 ± 0.05	2.71 ± 0.1	99.81
SRPK	4.04 ± 0.04	0.05	4.01	99.99

Table 3.29. Antibacterial activity of solar reflective paint filled with various antimicrobial agents for *S. aureus* strain

Result of bacteria array			Antibacterial activity R	Dead bacteria (%)
Incubation time	0 h	24 h		
Sample	Log (Average CFU/cm ²)	Log (Average CFU/cm ²)		
Control	4.06	4.04 ± 0.05	-	-
SRP1	4.06	0.58 ± 0.05	3.46 ± 0.1	99.96
SRPK	4.06	0.29 ± 0.04	3.75 ± 0.09	99.98

Observing the data in Tables 3.28 and Table 3.29, we see that after 24 hours of testing, the solar heat-reflective paint films were able to destroy most of the two tested bacterial strains, *E. coli* and *S. aureus* (> 99 %).

3.4.3.3. Antifungal ability of solar reflective paint

Table 3.30. Antifungal ability of solar reflective paint containing microbial agents

Sample	Evaluation time (day)	Percentage of surface area contaminated with fungi (%)	Antifungal level
SRP1	28	0	1
SRPK	28	0	0

Thus, the solar reflective paint containing the antimicrobial additive Ag-Zn/zeolite combined with OIT has good antibacterial ability against two tested bacterial strains (*E. coli* and *S. aureus*) and better fungal resistance than commercial antibacterial additives commonly used for water-based paints. On the other hand, Ag-Zn/zeolite and OIT do not greatly affect the ability of the paint to reflect light.

CONCLUSION

1. Organic surface modification of R-TiO₂ and ZrO₂ NPs using different coupling agents. The appropriate modification content for the above NPs is 3% wt (compared to the nanoparticles weight). The contents of TMSPM and GPTES grafted onto the surface of R-TiO₂ and ZrO₂ NPs are 0.122 and 0.068 mmol/g,

respectively. The organic modification process did not change the morphology, crystal structure and light reflection ability of the nanoparticles but improved the dispersion of the nanoparticles in water.

2. The appropriate content of organically modified R-TiO₂ and ZrO₂ NPs put into acrylic coating is 2 wt.%. Combining the above nanoparticles has significantly improved the properties of acrylic coating. Compared to a coating containing only one type of organically modified nanoparticle, this combined coating has 10% higher abrasion resistance, 10°C increase in heat resistance (decomposition starting temperature), and good weather resistance and light reflection improves by more than 20%.

3. Replacing R-TiO₂ microparticles with a mixture of organically modified nanoparticles (R-TiO₂ and ZrO₂) enhanced the solar heat reflection of the acrylic coating. This coating has the ability to reflect light better, increasing by about 5% compared to without nanoparticles. In addition, it also reduces the amount of water penetrating the paint film by up to 50% and increases cooling performance thanks to the use of paint film (reducing the surface temperature of the paint film by about 4 °C compared to a paint film without nanoparticles).

4. The presence of Ag-Zn/zeolite does not greatly affect the properties of the coating (heat resistance, abrasion resistance, weather resistance) but increases the bactericidal ability of the coating. After 24 hours, the coating containing 1% wt of Ag-Zn/zeolite can kill almost completely (> 99%) *E. coli* and *S. aureus* bacteria. organic compound - OIT does not have antibacterial ability against *E.coli* and *S.aureus* bacteria but has good fungal resistance (after 28 days of testing, the coating surface did not record fungal growth). The Ag-Zn/zeolite anti-microbial additive system combined with OIT does not affect the light reflection ability of the coating to reflect solar heat, but is resistant to *E.coli* and *S.aureus* (kills up to > 99 %) and good antifungal (after 28 days, no fungal growth).

NOVELTY CONTRIBUTIONS OF THE THESIS

1. Organic modification of R-TiO₂ nanoparticles and ZrO₂ nanoparticles with suitable coupling agents aims to enhance the compatibility and dispersibility of nanoparticles into the acrylic emulsion polymer matrix, consequently improving the coating properties.

2. Mix and combine additives, including organically modified nanoparticles, suitable antimicrobial agents like Ag-Zn/zeolite, and OIT, to create a synergistic effect aimed at enhancing various properties of the emulsion acrylic paint film, including mechanical properties, thermal stability, diffuse reflectivity of solar radiation, weather resistance, and antibacterial performance.

3. The environmentally friendly paint film having good solar heat reflection, antibacterial ability, and a long lifespan contributes to reducing cooling energy in construction and architectural projects, enhancing energy security, reducing CO₂ emissions/greenhouse gases, and improving building aesthetics.

LIST OF PUBLICATIONS FROM THE THESIS

1. **Phi Hung Dao**, Thuy Chinh Nguyen, Thi Lan Phung, Tien Dung Nguyen, Anh Hiep Nguyen, Thi Ngoc Lan Vu, Quoc Trung Vu, Dinh Hieu Vu, Thi Kim Ngan Tran, and Hoang Thai - Assessment of Some Characteristics and Properties of Zirconium Dioxide Nanoparticles Modified with 3-(Trimethoxysilyl) Propyl Methacrylate Silane Coupling Agent - Journal of Chemistry, Volume 2021, Article ID 9925355, 10 pages ([hNops://doi.org/10.1155/2021/9925355](https://doi.org/10.1155/2021/9925355)) (SCIE – IF: 3,241).

2. **Phi Hung Dao**, Tien Dung Nguyen, Thuy Chinh Nguyen, Anh Hiep Nguyen, Van Phuc Mac, Huu Trung Tran, Thi Lan Phung, Quoc Trung Vu, Dinh Hieu Vu, Thi Cam Quyen Ngo, Manh Cuong Vu, Vu Giang Nguyen, Dai Lam Tran, Hoang Thai - Assessment of some characteristics, properties of a novel waterborne acrylic coating incorporated TiO₂ nanoparticles modified with silane coupling agent and Ag/Zn zeolite - Progress in Organic Coatings 163 (2022) 106641 (<https://doi.org/10.1016/j.porgcoat.2021.106641>) (SCIE – IF: 6,13)

3. Thuy Chinh Nguyen, **Phi Hung Dao**, Quoc Trung Vu, Anh Hiep Nguyen, Xuan Thai Nguyen, Thi Ngoc Lien Ly, Thi Kim Ngan Tran, Hoang Thai - Assessment of characteristics and weather stability of acrylic coating containing surface modified zirconia nanoparticles - Progress in Organic Coatings 163 (2022) 106675 (<https://doi.org/10.1016/j.porgcoat.2021.106675>) (SCIE – IF: 6,13).

4. **Phi Hung Dao**, Thi Lan Phung, Anh Hiep Nguyen, Van Phuc Mac, Xuan Thai Nguyen, Thuy Chinh Nguyen, Quoc Trung Vu, Thi My Binh Dinh, Hoang Thai - Effect of organically modified titania and zirconia nanoparticles on characteristics, properties of coating based on acrylic emulsion polymer for outdoor applications – Journal of Applied Polymer Science, 140 (16) (2023), e53752 (<https://doi.org/10.1002/app.53752>) (SCIE – IF: 3,125).

5. Nguyen Thuy Chinh, Tran Thi Mai, **Dao Phi Hung**, Nguyen Anh Hiep, Nguyen Thi Thu Trang, Tran Huu Trung, Nguyen Xuan Thai, Dao Huu Toan, Dinh Thi My Binh, Thai Hoang - Characteristics of organic titanate modified titanium dioxide nanoparticles and its dispersibility in acrylic emulsion coating - Vietnam J. Chem., 2022, 60 (special issue), 116-124 (DOI: 10.1002/vjch.202200080) (Scopus, IF = 0,9, Q3).

6. Nguyen Thuy Chinh, **Dao Phi Hung**, Nguyen Xuan Thai, Nguyen Anh Hiep, Thai Hoang – Assessment of influence of modified zirconia nanoparticles content on the weather resistance of acrylic coating – Vietnam Journal of Science and Technology (Accepted to Vol. 61, 2023) (<https://doi.org/10.15625/2525-2518/16686>) (Scopus, Q4).

7. **Patent No. 35923**: Thai Hoang, **Dao Phi Hung**, Nguyen Thuy Chinh, Nguyen Anh Hiep, Tran Dai Lâm, Vu Quoc Trung, Dinh Thi My Binh – Method for producing a hybrid organic-inorganic coating system and the paint system obtained from the above method is heat resistant, abrasion resistant and antibacterial. (The patent was granted in accordance with Decision 26122/QĐ-SHTT.IP on 04 May 2023).